University „Babeş-Bolyai" Cluj-Napoca

Faculty of Biology and Geology

Chair of Mineralogy

Quartz andesites from the Oaş-Gutâi Neogene volcanic area (Romania)

Ph.D. Thesis Abstract

Scientific advisor

Prof. Univ. Dr. Corina Ionescu

Ph.D. Student

Geol. Maria Jurje

(b. Gabor)

Cluj Napoca

2012

CONTENTS

Ph.D. THESIS CONTENTS

Annexes

KEY WORDS: quartz andesites, Neogene, Oaş-Gutâi Mts., magmatic quartz, oscillatory zoned plagioclases, mineral chemistry, calc-alcaline volcanics, fractional crystallization, crustal assimilation, magma mixing.

INTRODUCTION

The Oaş-Gutâi Mts. are one of the major areas of interest for the geological and mining research, due to the complexity of the volcanism that developed in this area, and the associated mineralizations. In the evolution of the Neogene volcanism from the Oaş-Gutâi Mts., one of the most important stage is represented by the products of the quartz andesites. These rocks, characterized by the presence of the quartz phenocrysts, which were conventionally named „quartz andesites", are the research subject of this doctoral thesis.

The study focused on the emphasizing of the compositional, textural and chemical peculiarities of the quartz andesites, through petrographical and geochemical approaches. These peculiarities are the result of all the processes involved in petrogenesis, beginning with the source zone of formation of the parental magmas, and ending with the processes that took place in the crustal magma chambers. For the mineralogical characterization of these andesites, the optical microscopy studies were completed with electrone microprobe analysis. The geochemical study was based on ICP-MS analysis for major and minor elements, as well as rare earths elements.

CH. 1. HISTORY OF GEOLOGICAL RESEARCH IN THE AREA OF THE OAŞ - GUTÂI MTS.

The systematic research of the Oaş-Gutâi volcanic area beginns around the middle part of the 20th century. The first published papers focused on the structure types, rock types and the asssociated hydrothermal alterations, as well as on the gold-silver and complex sulphides minerallizations (Dimitrescu, 1954; Cioflică 1956; Rădulescu 1958; Giuşcă 1960; Ianovici *et al.* 1961; Sagatovici 1968; Rădulescu şi Borcoş 1969).

The general evolution of the Neogene volcanism from Oaş-Gutâi Mts. was presented in the papers published after 1970. Borcoş *et al.* (1973) present the evolution of the volcanism from the Gutâi Mts. following the cycles and erruption phases that succeded from the Badenian up to the Late Pliocene. The age of the volcanic products was established on the basis of the relationships with the paleontologically dated sedimentary formations. Edelstein *et al.* (1980, 1982) abandoned for the first time the division of the volcanism in cycles and phases. Based on the relationships with the paleontologically dated sedimentary deposits and on the spatial relationships between different volcanic products, the above authors established a sequence of the temporal evolution of the volcanism, from the Badenian up to the Pontian-Pliocene.

After 1980 a series of papers in which the igneous rocks from the Oaş-Gutâi Mts. were approached in the terms of their definition following the recommendations of the igneous rocks Systematic Commissions of the International Union of Geological Sciences (IUGS) was published. Important contributions regarding the detailed petrochemical, mineralogical-petrographical and structural-textural characterization, were also made (Kovacs *et al.,* 1987, 1989, 1992; Edelstein *et al.,* 1987, 1992; Fülöp *et al.*, 1991).

The geochronological data resulting from the radiometric datings (K-Ar and Ar-Ar) made on the igneous rocks and on the hydrothermal mineralizations lead to the reassessment of the evolution of the volcanism from the Oaş-Gutâi Mts. (Edelstein *et al.*, 1992a, 1993; Pécskay *et al.*, 1994, 1995a,b; Kovacs *et al.*, 1995, 1997a,b, 2010b; Fülöp, 2001; Lang *et al*.,1994). According to these data the volcanism from this area took place during the Badenian-Pannonian (15.4-7.0 Ma), and the hydrothermal activity took place during the Pannonian (11.5-7.9 Ma).

The most recent studies focused on deciphering the geotectonic evolution of the volcanic area Oaş-Gutâi and of the Carpathian-Pannonian region, as well as on the

petrogenetic processes (fractional crystallization, crustal assimilation, mixing and mingling magmas) involved in the genesis of the volcanics from the areas (Kovacs, 2002; Kovacs *et al*.,2010; Pécskay *et al*., 2006, 2009; Seghedi *et al*., 2004, 2005, Tischler *et al*., 2007).

CH. 2. GEOLOGICAL EVOLUTION OF THE CARPATHO-PANNONIAN REGION WITH SPECIAL REGARD ON THE NEOGENE VOLCANISM

The Carpahian chain is situated in the central and eastern part of Europe, and extends on a length of more than 1500 km, between the Eastern Alps and the Balkans. The formation of the chain and of the intra-carpathian basins is connected to the evolution of the Carpatho-Pannonian area during the Cenozoic, which was directly influenced by the convergence of the two major plates, the Eurasian plate and the African plate. The present configuration of this region is the result of the deformations suffered by the two continental blocks and the rifts between them (Csontos, 1995; Peresson and Decker, 1997).

According to the recent models of the geotectonic evolution of the Carpatho-Pannonian region, the lithospheric plates involved in the convergent processes responsible for the Miocene subduction are the East European Plate to the east, and the Alcapa and Tisia (Kovács, 1982) microplates to the west (Fig. 2.1). The last plate is also named „Tisza-Dacia" (Csontos *et al.*, 1992, Csontos, 1995), respectively „Tisia-Getia" (Seghedi *et al.*, 1998). The Alcapa and Tisia microplates are separated by the „Mid-Hungarian Line" – a major fault, with transcrustal character (Csontos and Nagymarosy, 1998). While moving towards east and north-east, the two blocks, Alcapa and Tisia, also suffered rotation and translation movements (Marton *et al.*, 1992; Pătraşcu *et al.*, 1994; Panaiotu *et al.*, 1996).

The calc-alkaline magmatism from the Carpatho-Pannonian area is mostly located along the north-eastern margin of the Alcapa and Tisia plates. The volcanic arc, from the inner part of the Carpathian chain has a Neogene-Quaternary age, and is the result of the complex subduction, collision, post-collision and extention processes (Szabó et al., 1992; Csontos, 1995; Lexa and Konečny, 1998; Mason et al., 1998; Nemčok et al., 1998; Seghedi et al., 1998; Seghedi *et al*., 2004, 2005; Pécskay *et al.*, 2004, 2006, 2009; Tischler *et al*., 2007).

According to the new evolutional model developed by Kovacs (2002), Oaş-Gutâi volcanic arc was generated by magmatic processes developed within the Alcapa microplate

(partly also within Tisia) due to the subduction of the East European plate beneath them. The beginning of the arc-type volcanism in the Oaş-Gutâi Mts. area (13.4-13.2 Ma ago) took place at about 6-7 Ma from the beginnig of the Miocene subduction (about 20-22 Ma ago), during the Early Miocene respectively.

The volcanism from the Oaş-Gutâi Mts. has a calc-alkaline character, typical for the subduction areas, and was activ all along the sinking and consuming of the oceanic lithosphere. The paroxysm was recorded just a little before the collision of the continental plates (considered to take place about 10-9 Ma ago). The volcanic arc generated at the border of the Alcapa and Tisia microplates is of continetal margin type. The geochemical and isotopical study of the volcanic rocks from the Gutâi Mts. (Kovacs, 2002) emphasized the similitude both with other segments from the Carpathian volcanic arc – first of all with the Călimani-Gurghiu-Harghita Mts., and with other arcs from recent and present day subduction zones.

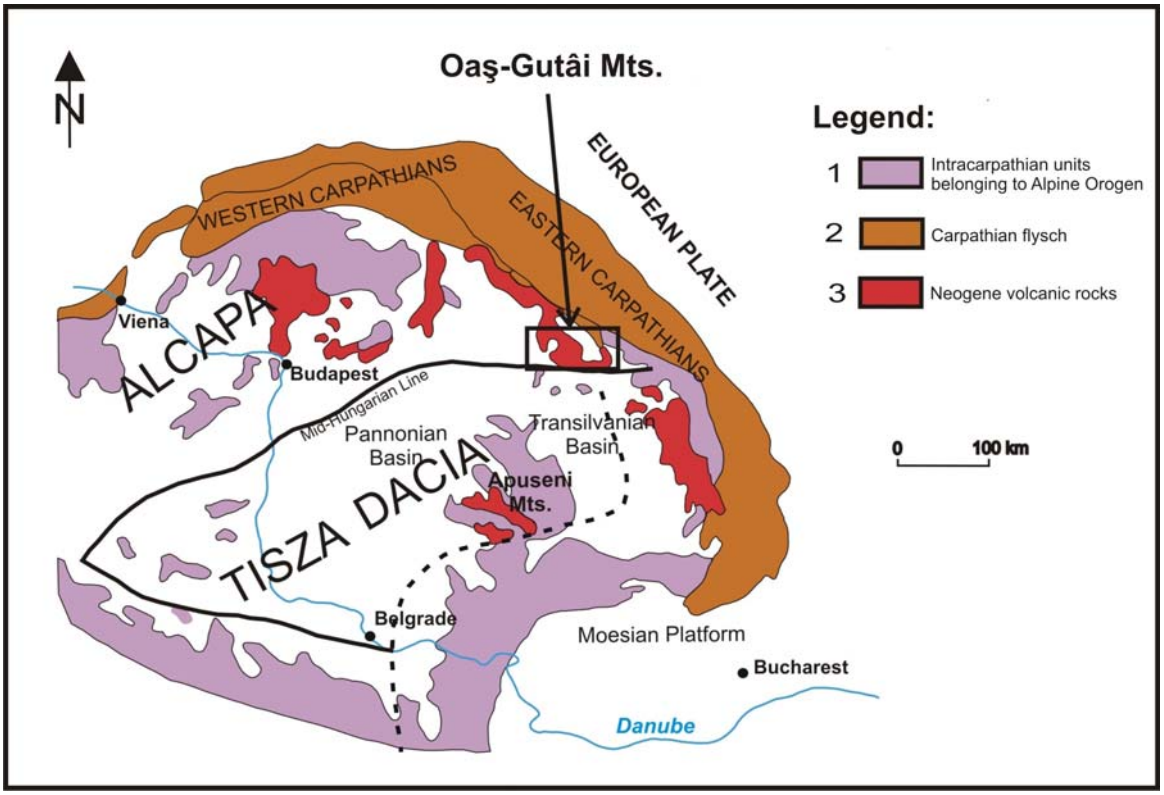

Fig. 2.1. Geotectonic sketch map of Carpathian-Pannonian region (Săndulescu, 1988 and Csontos *et al.,* 1992); location of Oaş-Gutâi Mts. (modified after Kovacs, 2002).

CH. 3. GEOLOGICAL STRUCTURE OF THE OAŞ-GUTÂI MTS. AND THE EVOLUTION OF THE NEOGENE VOLCANISM

The Oaş-Gutâi Mts. are the north-western segment of the Eastern Carpathians from the teritory of Romania, and are a segment of the Neogene-Quaternary volcanic range which extends from the Western Carpathians (in Slovakia) to the curvature of the Carpathians (in Romania). In the overall structure of the volcanic mountains Oaş-Gutâi, three main geological units can be defined: the pre-volcanic basement, the Neogene sedimentary cover and the Neogene igneous rocks.

3.1. The structure of the pre-volcanic basement

The pre-volcanic basement is made of Precambrian/Paleozoic metamorphic formations which belong to the major units of the Inner and Median Dacides, and flysch sedimentary deposits arranged in overthrusting nappes, belonging to the Piennides units (Săndulescu, 1984, 1993). The structural elements that have left their mark on the overall structure of the pre-volcanic basement are represented by the faults system Bogdan Vodă - Dragoş Vodă (Săndulescu, 1984), Gutâi fault and a series of other secondary faults oriented E-V, NV-SE and NE-SV.

3.2. The Neogene sedimentary deposits

During the Neogene, the volcanic activity developed synchronously with the sedimentation processes, between the volcanic deposits and the sedimentary ones direct relationships being frequently recorded. The sedimentation began during the Middle Miocene (Lower Badenian) and continued, with local and regional interruptions, until the end of the Pannonian. The Neogene sedimentary cover is represented by Badenian, Sarmatian and Pannonian deposits. Lithologically, they consist of clays, marls and sandstones with microconglomeratic intercalations and limestones.

3.3. Evolution of the Neogene volcanism from the Oaş-Gutâi Mts.

The Neogene igneous rocks are the most significant deposits from the Oaş-Gutâi Mts. and are typical for the calc-alkaline series, also including, besides the andesites and basaltic andesites which are predominant, dacites, rhyolites and basalts. The volcanic

activity from the Oaş-Gutâi Mts. developed between the Badenian and the Pannonian. Two types of volcanism were asserted: an acidic extentional /"back-arc" volcanism and an intermediate arc-type volcanism (Kovacs & Fülöp, 2003).

In the Oaş Mts. the volcanism developed from the Upper Badenian until the Pannonian, with the temporal and spatial overlapping of the different volcanic products. The buried acidic volcanism, with explosive character, developed in the central part of the Oaş Mts. during the Upper Badenian-Lower Sarmatian (Fülöp & Crihan, 2002). The intermediate volcanism, with extrusive and intrusive character, represents the main stage of the volcanic activity, and is developed in the whole area of the Oaş Mts. during the Sarmatian-Pannonian, between 12.9-9.5 Ma (Kovacs *et al.*, 1997a). It is represented by rhyolites, dacites, quartz andesites and pyroxene andesites (Fig. 3.1) as lava flows and extrusive domes (Kovacs & Fülöp, 2002).

In the Gutâi Mts. the volcanic activity was extremely complex (Fig. 3.1) and developed during the Badenian-Pannonian interval (15.4-6.9 Ma). The onset of the volcanic activity had been in Badenian by the calc-alkaline acid volcanism (15.4 Ma – Fülöp, 2002) followed by the main intermediate volcanic stage, with the greatest temporal and spatial extent. The Badenian volcanism is represented by ignimbrites and their associated volcaniclastic deposits (Fülöp & Crihan, 1995; Fülöp, 2003). The intermediate volcanism developed during the Sarmatian-Pannonian interval, respectively between 13.4-6.9 Ma (Edelstein *et al.*, 1992 a, 1993; Pécskay *et al.,* 1994, 1995). The Sarmatian volcanics (13.4 – 12.1 Ma - Edelstein *et al.,* 1992 a; Pécskay *et al.,* 1994) are predominantly represented by basaltic andesites and pyroxene andesites, as well as by pyroxene dacites, and are extended in the south-western and south-eastern parts of the Gutâi Mts. (Fig. 3.1). The paroxysm of the volcanism took place during the Pannonian (11.6-9.0 Ma - Edelstein *et al.*,1992a; Pécskay *et al.,*1994,1995), when most of the volcanics from the Gutâi Mts were emplaced. The succession of the Pannonian volcanics is as follow: pyroxene andesites lava flows, pyroxene and amphibole lava flows associated with volcaniclastites (predominantly hyaloclastites), basaltic andesites and pyroxene andesites lava flows, pyroxene andesites with biotite and dacites with biotite as extrusive domes. Some small intrusive bodies of pyroxene basalts (8.1 – 6.9 Ma - Edelstein *et al.,*1993) ceased the volcanism from the Gutâi Mts.

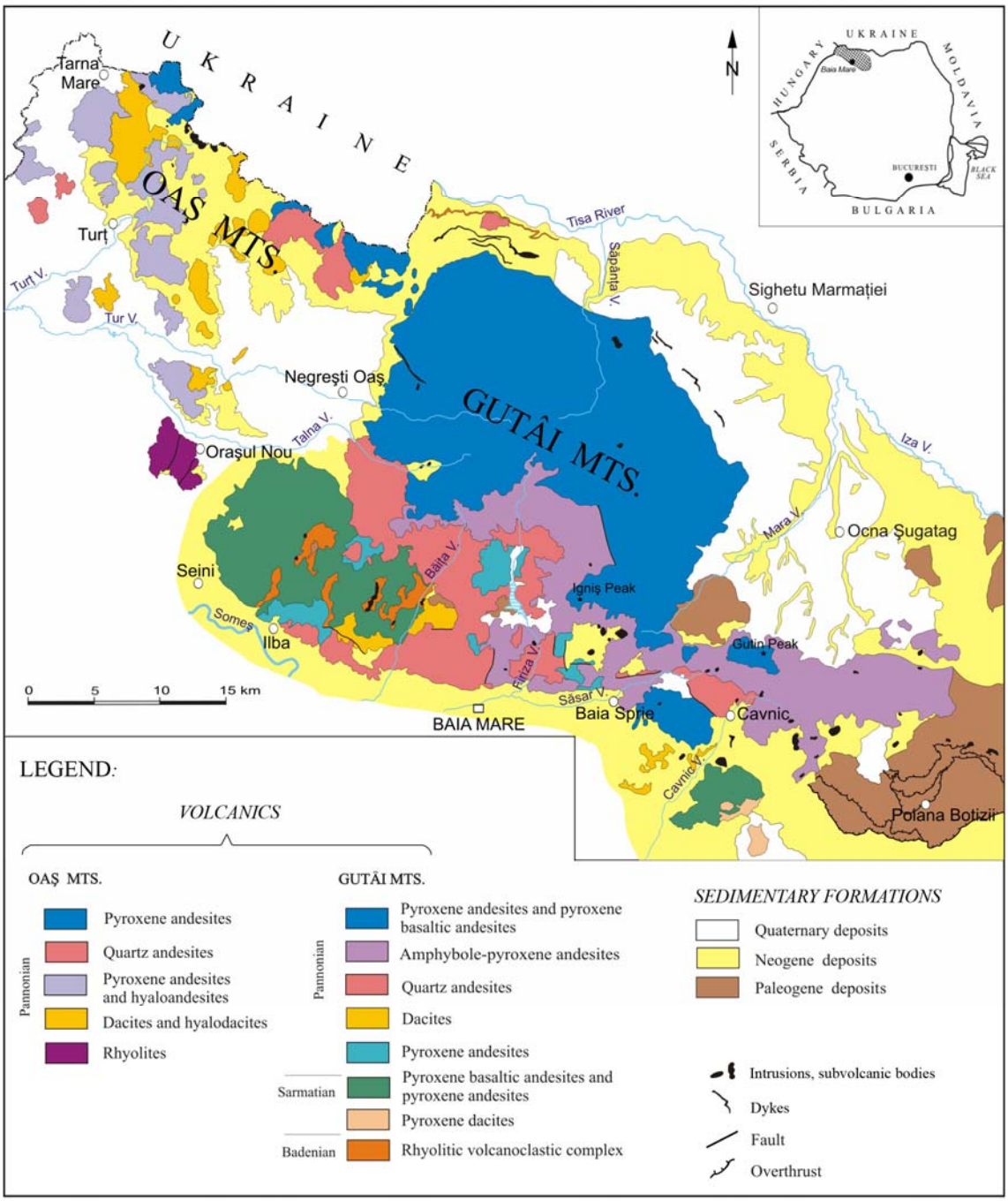

Fig. 3.1. Simplified geological map of the Oaş-Gutâi Mts. (after Gabor et al. 1999[1] şi Edelstein et al , 1980[2])

[1] Gabor, M., Kovacs, M., Edelstein, O., Iştvan, D., Bernad, A., 1999. Geological map of the Oaş-Gutâi-Ţibleş Mts. 1:25000 scale. S.C. IPEG Maramures, Baia Mare. (in Romanian, unpublished).

[2] Edelstein, O., Iştvan, D., Cojocea, C., Weisz, G., Bernad, A., Stan, D., Kovacs, M., 1980. Geological map of the Oaş-Gutâi-Ţibleş Mts. 1:25000 scale. S.C. IPEG Maramures, Baia Mare. (in Romanian, unpublished).

Important hydrothermal mineralizations of epithermal type, predominantly polymetallic and gold-silver are associated with the Neogene volcanism from the Oaş-Gutâi Mts. The metallogenetic activity from the Oaş-Gutâi Mts. took place between 11.6-7.9 Ma (Lang *et al.*, 1994; Kovacs *et al.*, 1997b).

CH. 4. MATERIALS AND ANALITICAL METHODS

The polarized light microscopic study was performed on 95 thin sections (65 from Gutâi Mts. and 30 from Oaş Mts.) using a Jenapol microscope.

The chemical composition of the minerals from the quartz andesites was performed on 11 samples using an electrone microprobe at the Salzburg University (Austria). 1827 punctual analyses were made, as follows: 786 on plagioclase feldspars, 212 on orthopyroxenes, 308 on clinopyroxenes, 55 on amphiboles, 91 on accessory minerals (Ti-magnetite and ilmenite), 113 on the groundmass and 262 on secondary minerals.

On 26 samples were performed geochemical analysis for major, minor and rare earths elements, by ICP-MS methode, at the Acme Analytical Laboratories Ltd. Vancouver (Canada).

CH. 5. MINERALOGY AND PETROLOGY OF THE PANNONIAN QUARTZ ANDESITES FROM THE OAŞ-GUTÂI MTS.

The quartz andesites are rocks with porphyritic texture, with phenocrysts of plagioclase feldspars (18-30%), pyroxenes (2-14%), amphiboles (3-10%) and quartz (1-6.5%) in a hyalopillitic, intersertal or holocrystaline groundmass.

5.1. Plagioclase feldspars

Plagioclase feldspars are the main constituents of the quartz andesites and are present both as phenocrysts and as microlites in the groundmass. They generally show euhedral and, subordinately, subhedral and anhedral outline and their sizes varies between 1 and 8 mm. The plagioclase feldspars are intergrown, twinned (Fig. 5.1a), with intense oscillatory zoning and with frequent sieve textured cores or such textures developed as concentric bands towards the rims (Fig. 5.2b).

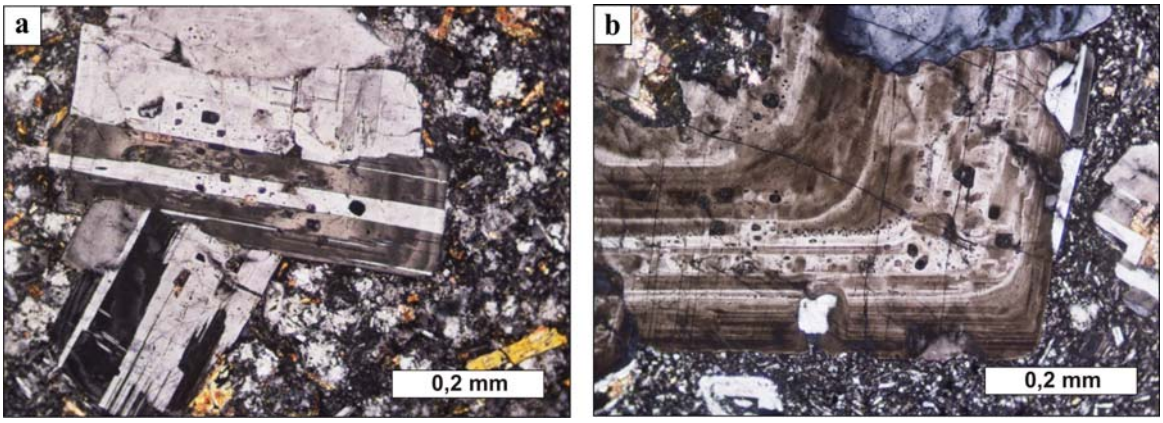

Fig. 5.1. Microphotographs of plagioclase phenocrysts from the quartz andesites. a) Intergrown plagioclase feldspars with polysynthetic twinnings (Sample 7572-M); b) Oscillatory zoned plagioclase phenocryst, with sieve texture zones and glass inclusions (Sample 7554-M). P+.

On the whole, the anortite content of the plagioclase feldspars varies in a very large interval, between 26.1 and 92.9%, corresponding to the andezine-labradorite-bytownite members of the series, and subordinately to oligoclaze and anortite, according to the classification diagram Ab-An-Or (Fig. 5.2).

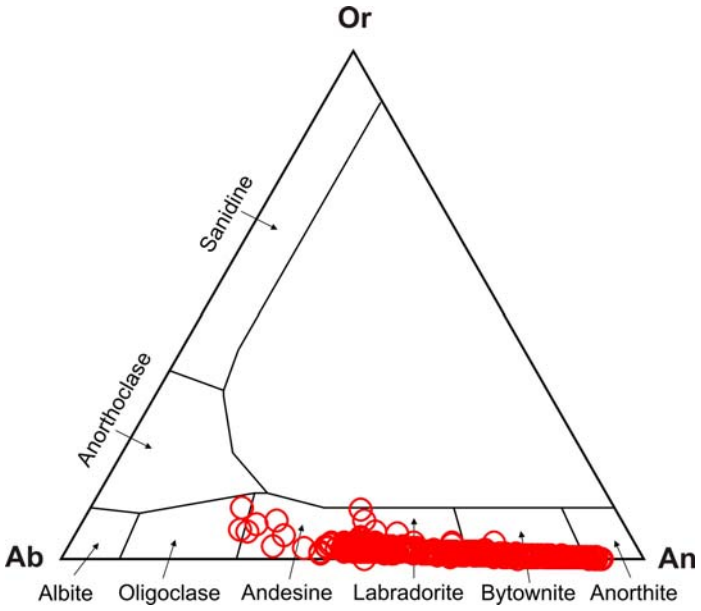

Fig. 5.2. Distribution of the composition of the plagioclase feldspars from the quartz andesites in the Ab-An-Or classification diagram

Most of the plagioclase phenocrysts show oscillatory zoning, both normal and reverse. Generally, the plagioclase feldspars from the quartz andesites show typical normal zoning, with the decrease of the An content from the core toward the rim of the crystal (Fig. 5.3a,b). In the core the An content has values between 72-90%, and in the rim 45-50% (table 1, sample 7567-M, analysis points 15-21).

In the case of the reverse zoning of the plagioclase feldspars (Fig. 5.3c,d), an increase of the An content from the core of the phenocrysts rimward is recorded. In the acidic cores, generally of great sizes, the An content, is around 50%, while in the much more basic rims it can reach values around 75-85% (table 1, sample 7566-M, analysis points 3-9).

In most of the oscillatory zoned plagioclase feldspars many recurences were recorded (Fig. 5.3e,f), and the difference between the An contents from the different zones of one phenocryst varies between 10 and 40% (table 1, sample 7572, analysis points 1-8).

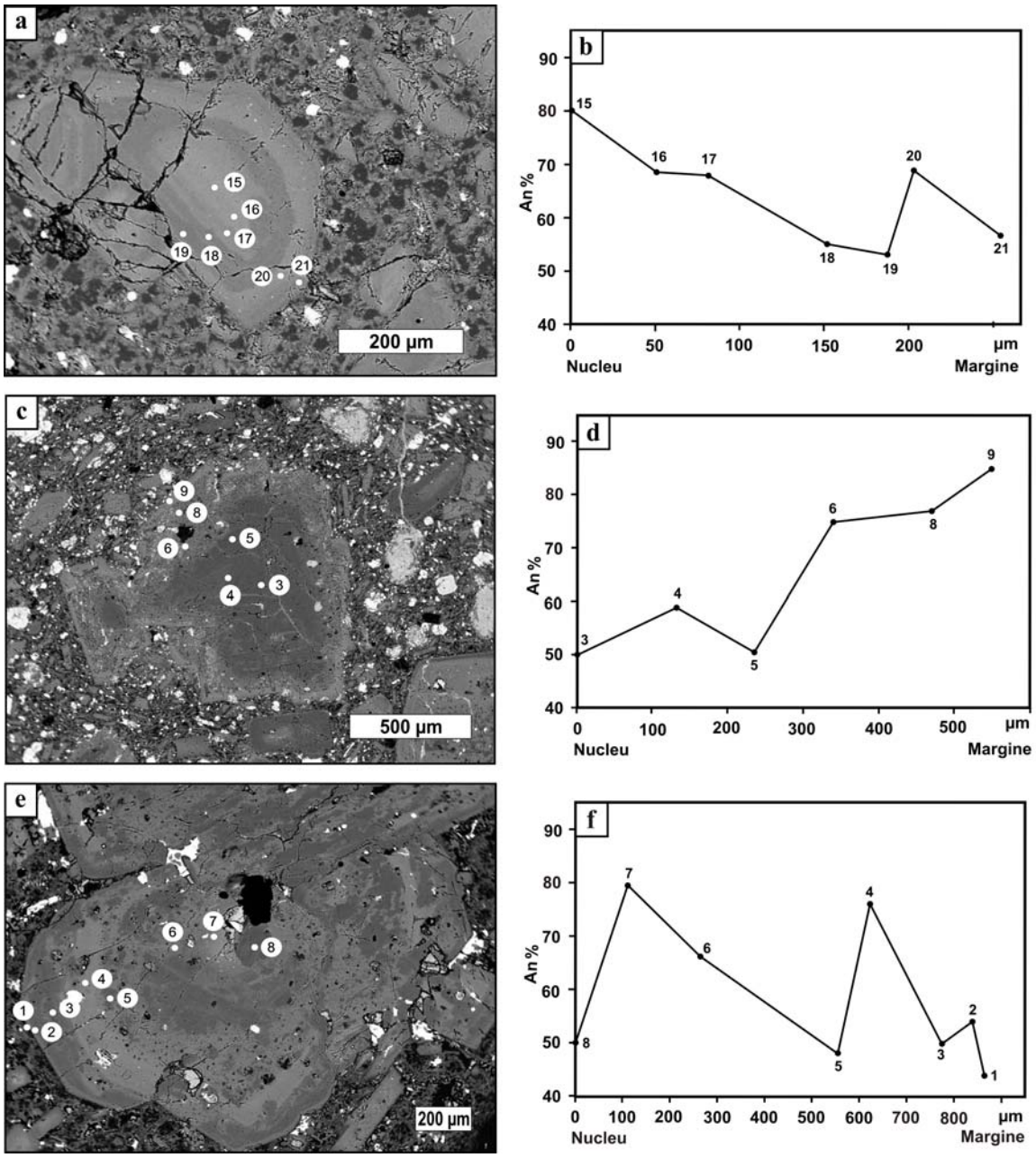

Fig. 5.3. BSE images of zoned plagioclase felspars from quartz andesites. a) Normally zoned phenocryst with a recurrence in the rim. Sample 7567-M, microanalysis points 15-21; b) Variation of An content in the phenocryst from image a; c) Reversely zoned phenocryst with corroded rim. Sample 7566-M, microanalysis points 3-9; d) An content variation of the phenocryst from image c; e) Zoned feldspar with acidic core and recurrence zones. Sample 7572-M, microanalysis points 1-8; f) An content variation of the phenocryst from image e.

Table 1. Selected microprobe analyses for plagioclase feldspar from quartz andesites (Oaş-Gutâi Mts.). Structural formulas are calculated on the basis of 8O, according to Deer *et al.* (1992). Fe_{TOTAL} as Fe^{2+}.

Sample	7566-M						7567-M						
Point	3	4	5	6	8	9	15	16	17	18	19	20	21
SiO_2	56,09	53,98	56,31	49,81	48,79	47,39	49,15	52,33	52,44	55,37	56,13	52,07	54,95
TiO_2	0,00	0,02	0,00	0,02	0,02	0,00	0,01	0,02	0,01	0,01	0,04	0,05	0,03
Al_2O_3	27,40	28,98	27,45	31,33	31,75	33,00	31,97	30,03	29,64	27,69	27,23	29,35	27,77
FeO	0,23	0,26	0,24	0,51	0,58	0,85	0,19	0,24	0,29	0,25	0,20	0,60	0,49
MnO	0,00	0,00	0,00	0,00	0,04	0,05	0,00	0,00	0,00	0,00	0,00	0,00	0,00
MgO	0,00	0,01	0,01	0,04	0,06	0,00	0,03	0,00	0,03	0,02	0,01	0,07	0,02
CaO	10,46	12,08	10,41	15,07	15,68	17,24	16,28	14,03	13,85	11,39	10,86	13,96	11,58
Na_2O	5,46	4,50	5,37	2,73	2,51	1,65	2,21	3,45	3,54	4,96	5,16	3,41	4,74
K_2O	0,36	0,27	0,41	0,14	0,14	0,05	0,08	0,14	0,16	0,25	0,28	0,14	0,25
Total	100,00	100,10	100,22	99,69	99,57	100,31	99,95	100,25	99,98	99,94	99,94	99,70	99,86
Si	2,53	2,44	2,53	2,29	2,25	2,18	2,25	2,37	2,38	2,50	2,53	2,38	2,49
Al	1,45	1,54	1,45	1,69	1,72	1,79	1,72	1,60	1,59	1,47	1,45	1,58	1,48
Ti	0,00	0,00	0,00	0,00	0,00	0,00	0,00	0,00	0,00	0,00	0,00	0,00	0,00
Fe^{2+}	0,01	0,01	0,01	0,02	0,02	0,03	0,01	0,01	0,01	0,01	0,01	0,02	0,02
Mn	0,00	0,00	0,00	0,00	0,00	0,00	0,00	0,00	0,00	0,00	0,00	0,00	0,00
Mg	0,00	0,00	0,00	0,00	0,00	0,00	0,00	0,00	0,00	0,00	0,00	0,01	0,00
Ca	0,51	0,59	0,50	0,74	0,77	0,85	0,80	0,68	0,68	0,55	0,53	0,68	0,56
Na	0,48	0,39	0,47	0,24	0,22	0,15	0,20	0,30	0,31	0,44	0,45	0,30	0,42
K	0,02	0,02	0,02	0,01	0,01	0,00	0,00	0,01	0,01	0,01	0,02	0,01	0,01
Total cations	4,99	4,99	4,99	4,99	5,01	5,00	4,98	4,98	4,98	4,98	4,98	4,98	4,98
Anorthite	**50,3**	**58,8**	**50,6**	**74,8**	**76,9**	**85,0**	**80,0**	**68,6**	**67,8**	**55,1**	**52,9**	**68,8**	**56,7**
Albite	**47,6**	**39,6**	**47,1**	**24,4**	**22,3**	**14,7**	**19,6**	**30,6**	**31,3**	**43,5**	**45,5**	**30,4**	**41,9**
Orthoclase	**2,1**	**1,6**	**2,3**	**0,8**	**0,8**	**0,3**	**0,4**	**0,8**	**0,9**	**1,4**	**1,6**	**0,8**	**1,4**

Table 1. Continued.

Sample	**7572-M**							
Point	1	2	3	4	5	6	7	8
SiO_2	57,89	55,57	56,34	49,32	56,50	51,72	47,43	54,60
TiO_2	0,02	0,00	0,01	0,00	0,00	0,00	0,01	0,02
Al_2O_3	26,81	28,54	27,82	32,39	27,74	30,35	32,76	28,07
FeO	0,38	0,24	0,23	0,33	0,20	0,23	0,30	0,20
MnO	0,00	0,02	0,02	0,00	0,00	0,03	0,00	0,00
MgO	0,02	0,02	0,00	0,01	0,00	0,01	0,01	0,01
CaO	9,09	10,84	10,19	15,36	9,93	13,30	16,13	10,44
Na_2O	6,25	5,02	5,46	2,59	5,65	3,64	2,22	5,48
K_2O	0,22	0,25	0,29	0,08	0,30	0,16	0,08	0,27
Total	100,67	100,53	100,38	100,10	100,32	99,48	98,97	99,12
Si	2,58	2,49	2,53	2,25	2,53	2,36	2,20	2,49
Al	1,41	1,51	1,47	1,74	1,46	1,63	1,79	1,51
Ti	0,00	0,00	0,00	0,00	0,00	0,00	0,00	0,00
Fe^{2+}	0,01	0,01	0,01	0,01	0,01	0,01	0,01	0,01
Mn	0,00	0,00	0,00	0,00	0,00	0,00	0,00	0,00
Mg	0,00	0,00	0,00	0,00	0,00	0,00	0,00	0,00
Ca	0,43	0,52	0,49	0,75	0,48	0,65	0,80	0,51
Na	0,54	0,44	0,48	0,23	0,49	0,32	0,20	0,48
K	0,01	0,01	0,02	0,00	0,02	0,01	0,01	0,02
Total cations	4,99	4,98	4,98	4,99	4,99	4,99	5,01	5,01
Anorthite	**44,0**	**53,7**	**49,8**	**76,3**	**48,4**	**66,3**	**79,6**	**50,4**
Albite	**54,7**	**44,9**	**48,4**	**23,3**	**49,8**	**32,8**	**19,9**	**48,0**
Orthoclase	**1,3**	**1,4**	**1,7**	**0,4**	**1,7**	**0,9**	**0,5**	**1,6**

5.2. Pyroxenes

The pyroxenes are represented by orthopyroxenes and clinopyroxenes, the ratio between them being variable. They are as euhedral and subhedral crystals, predominantly prismatic, with small sizes (1-4 mm), sometimes polysyntetically twinned (Fig. 54a) and frequently as clusters (Fig. 5.4b). The clinopyroxenes are generally fresh, while the orthopyroxenes are partly or totally substituted by secondary minerals (carbonates, clorites, opaque minerals).

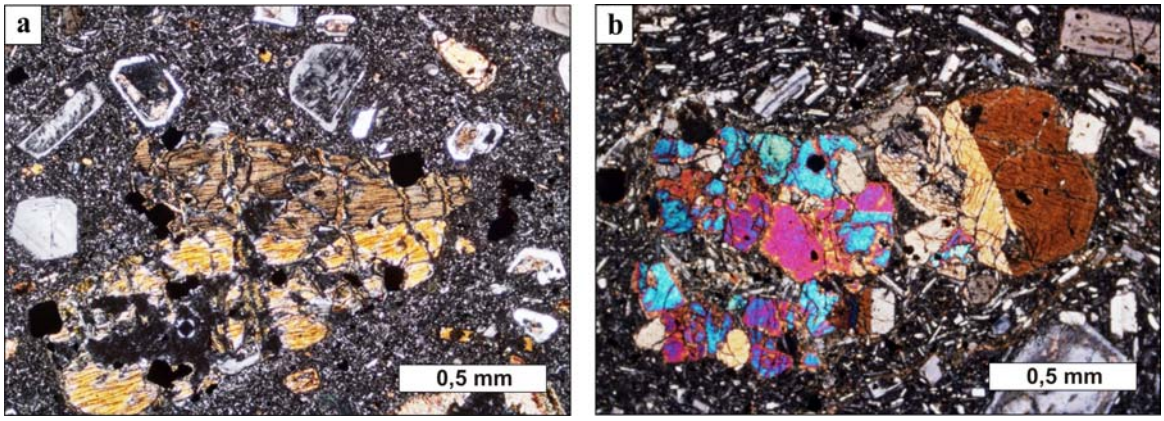

Fig. 5.4. Microphotographs of pyroxene phenocrysts from the quartz andesites. a) Twinned orthopyroxene phenocrysts (Sample 7554-M); b) Glomeroporphyritic clusters of clino- and orthopyroxene phenocrysts (Sample 7627-M). P+.

The clinopyroxenes are represented mostly by augite, and subordinately by diopside, and the orthopyroxenes by enstatite and subordinatly by ferosilite, according to the pyroxene classification diagram (Morimoto, 1989) (Fig. 5.5). The augite has the following composition: wollastonite (Wo): 30.3-44.9%, enstatite (En): 35.8-51.4%, ferrosilite (Fs): 8.1-24.5 %. The diopside composition: wollastonite: 45.1-50.5%, enstatite: 33.8-45.7% and ferrosilite: 8.5-17.1%. The magnesium number (Mg# = Mg/Mg+Fe) of the clinopyroxenes varies between 65.6 and 87.0. Orthopyroxenes composition is as follows: wollastonite: 1.3-8.4%, enstatite: 39.5-71.4% and ferrosilite: 21.6-58.6%. Mg# varies between 44.0 and 79.0.

Most of the clinopyroxene phenocrysts are zoned. A part of the clinopyroxene phenocrysts show normal zoning, in which case an enrichment in Mg occurs in the core of the crystals and it decreases towards the rim of the crystals, where an enrichment in Fe takes place (Fig. 5.6a). The En content vary between 43 and 45% in the core, and decreases in the rim till around 41.0%, while the Fs content increases from values of 9.3-10.3% in the core, to 16.6% in the rim of the crystal. The magnesium number (Mg #)

decreases in these clinopyroxene phenocrysts from 82-84 in the core, to 74 in the rim. This decrease is not continous though, in most cases recurrence zones occur, as results from the large variation interval (between 75 and 84) of the Mg# from the intermediate zone (table 2, sample 7566-M, microanalysis points 1-7). In other cases, a reverse zoning of the clinopyroxenes (Fig. 5.6b) was noticed, in which the Mg content increseas towards the rim of the phenocrysts, while the Fe content increseas towards their core. The En content in their core has values between 34.3 and 36.7%, and in the rim increases till 45.2%. The Fs content decreseas from high values of 14.7-17.1% in the core, till 10.8-12.3% in the rim. In this case it also to be noticed the presence of some significant recurrences illustrated by successive increases and decreases of the Mg content and Fe. The values of the magnesium number confirm this tendency, as it has values between 69 and 73 in the core, and reaches 80 in the rim, while in the intermediate zone Mg# varies between much wider limits, respectively between 71 and 80 (table 2, sample 7568-M, microanalysis points 1-8).

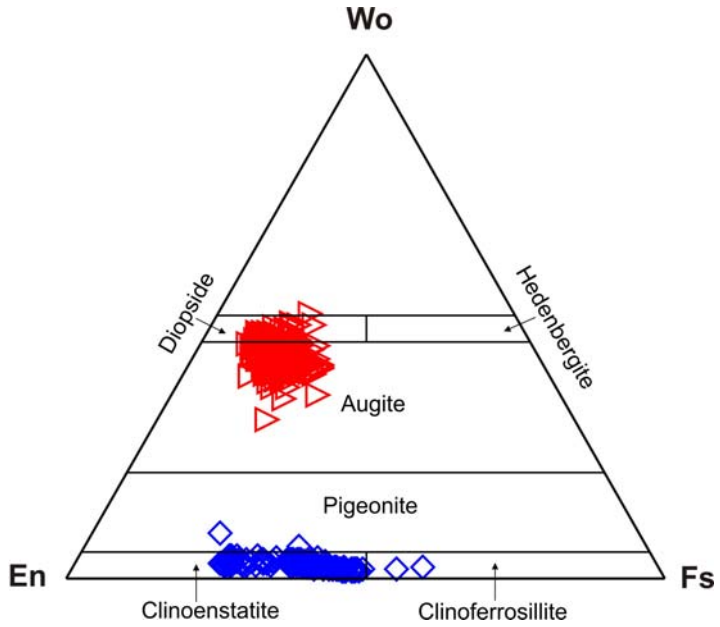

Fig. 5.5. Distribution of the composition of the orthopyroxenes and clinopyroxenes from the quartz andesites in the Wo-En-Fs classification diagram (Morimoto 1988). Legend: red triangle-clinopyroxenes; blue rhomb-orthopyroxenes.

The orthopyroxenes are either as homogenous or zoned crystals. In the case of the normally zoned crystals (Fig. 5.6c) an enrichment in Mg in the core and an empowerishment towards the rim can be noticed. Fe has a reverse variation, with lower contents in the core of the crystals and a higher content towards the rim. Thus, the En content in the core has a value of 69.5% and decreases till 55.2% in the rim, while the Fs

content increases from 27.7% to 42.7%. The magnesium number (Mg#) has high values (74.1) in the core and much lower values (59.8) in the rim (table 3, sample 7568-M, microanalysis points 19-22).

In the reversly zoned crystals (Fig. 5.6d), an increase of the Mg content from the core towards the rim can be noticed, as well as an enrichment in Fe in their core, and the magnesium number increases from the core towards the rim. The En content in the core is 52.4% and increases till 60% in the rim, and the Fs content decreases from 45.9% till 37.3%. The magnesian number increases from 57 in the core to 65 in the rim (table 3, sample 7571-M, microanalysis points 13-18). In this case recurence areas appear, with succesive increases and decreases of En and Fs within the same crystal. However, homogeneous, unzoned crystals also occur, within which the Mg and Fe contents show insignificant variations.

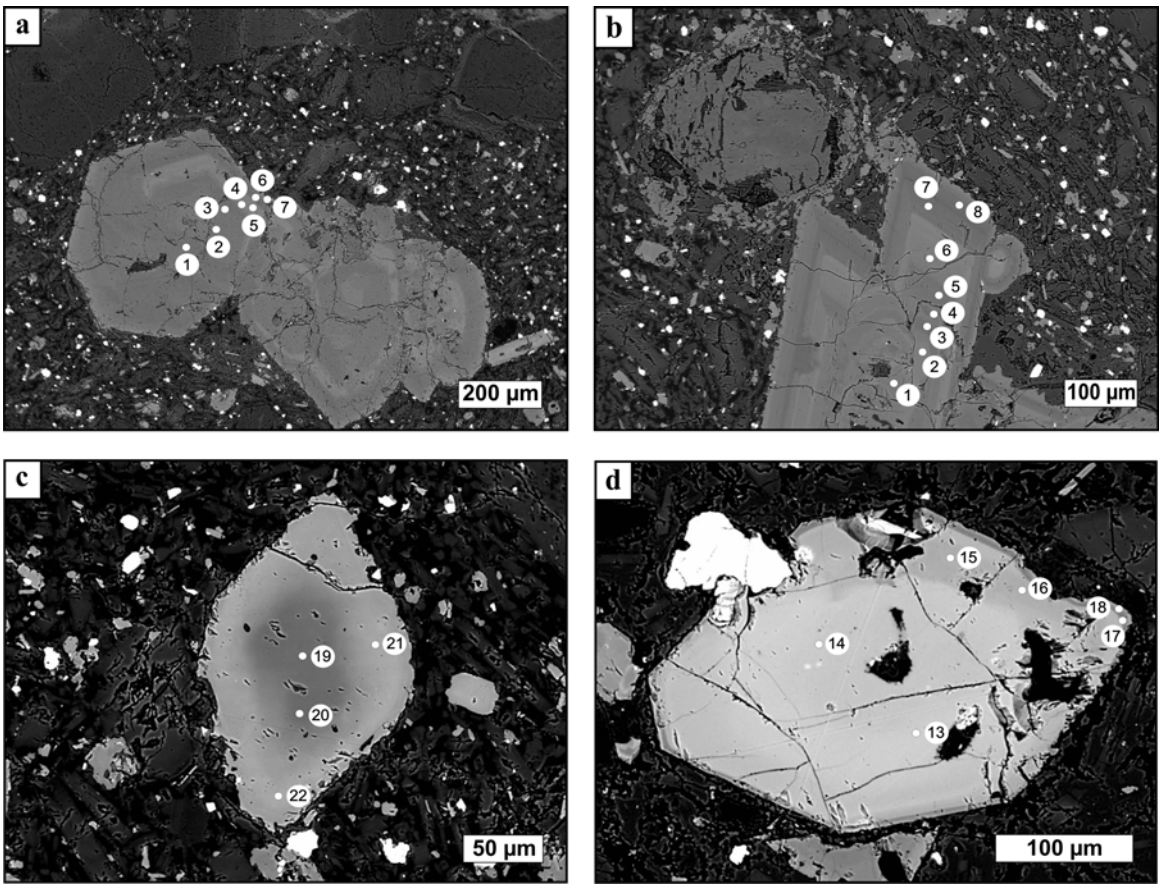

Fig. 5.6. BSE images of pyroxenes from the quartz andesites. a) Normally zoned clinopyroxene phenocrysts (Sample 7566-M, microanalysis points 1-7); b) Reversely zoned subhedral clinopyroxene phenocryst, with Fe rich core (sample 7568-M, microanalysis points 1-8); c) Normally zoned orthopyroxene with resorbed rim (Sample 7568-M, microanalysis points 19-22) ; d) Orthopyroxene crystal with reverse zoning and recurrence zones (Sample 7571-M, microanalysis points 13-18).

Table 2. Selected microprobe analyses for clinopyroxene from quartz andesites (Oaş-Gutâi Mts.). Structural formulas are calculated on the basis of 6O, according to Cawthorn & Collerson (1974). Fe_{TOTAL} as Fe^{2+}.

Sample	7566-M							7568-M							
Point	1	2	3	4	5	6	7	1	2	3	4	5	6	7	8
SiO_2	51,45	50,52	52,63	53,12	53,53	52,84	53,73	48,82	47,78	52,16	50,69	51,25	50,50	52,25	52,70
TiO_2	0,57	0,77	0,46	0,51	0,26	0,40	0,32	0,93	1,02	0,54	0,64	0,61	0,56	0,50	0,51
Al_2O_3	4,78	5,54	3,63	2,32	1,53	3,01	0,97	5,96	6,97	3,10	4,04	3,75	3,93	3,34	3,04
FeO	5,78	6,24	5,70	10,01	9,82	5,92	10,09	8,64	9,93	6,84	7,92	7,72	9,30	6,67	7,52
MnO	0,08	0,10	0,13	0,33	0,45	0,15	0,32	0,21	0,16	0,13	0,13	0,09	0,15	0,08	0,20
MgO	15,24	14,71	15,76	15,24	15,03	16,41	14,82	12,39	11,33	14,50	12,79	13,53	11,51	14,34	15,82
CaO	22,34	22,37	22,21	19,57	20,39	21,78	20,10	22,71	22,26	22,49	22,97	22,81	23,94	23,21	20,61
Na_2O	0,15	0,15	0,12	0,16	0,23	0,14	0,33	0,20	0,28	0,20	0,16	0,18	0,18	0,16	0,14
Cr_2O_3	0,36	0,33	0,23	0,00	0,00	0,21	0,03	0,00	0,00	0,01	0,00	0,03	0,00	0,05	0,07
Total	100,74	100,73	100,87	101,26	101,26	100,87	100,71	99,87	99,72	100,01	99,38	99,99	100,08	100,60	100,61
Si	1,87	1,85	1,92	1,95	1,97	1,92	1,99	1,82	1,80	1,93	1,90	1,90	1,90	1,92	1,93
Al^{IV}	0,13	0,15	0,08	0,05	0,03	0,08	0,01	0,18	0,21	0,07	0,10	0,10	0,11	0,08	0,07
Al^{VI}	0,08	0,09	0,07	0,05	0,03	0,05	0,03	0,09	0,10	0,06	0,08	0,07	0,07	0,07	0,06
Ti	0,02	0,02	0,01	0,01	0,01	0,01	0,01	0,03	0,03	0,02	0,02	0,02	0,02	0,01	0,01
Fe^{2+}	0,18	0,19	0,17	0,31	0,30	0,18	0,31	0,27	0,31	0,21	0,25	0,24	0,29	0,21	0,23
Mn	0,00	0,00	0,00	0,01	0,01	0,01	0,01	0,01	0,01	0,00	0,00	0,00	0,01	0,00	0,01
Mg	0,83	0,80	0,86	0,83	0,82	0,89	0,82	0,69	0,63	0,80	0,72	0,75	0,64	0,79	0,87
Ca	0,87	0,88	0,87	0,77	0,80	0,85	0,80	0,91	0,90	0,89	0,92	0,91	0,96	0,91	0,81
Na	0,01	0,01	0,01	0,01	0,02	0,01	0,02	0,02	0,02	0,01	0,01	0,01	0,01	0,01	0,01
Cr	0,01	0,01	0,01	0,00	0,00	0,01	0,00	0,00	0,00	0,00	0,00	0,00	0,00	0,00	0,00
Total cations	4,00	4,00	4,00	4,00	4,00	4,00	4,00	4,00	4,00	4,00	4,00	4,00	4,00	4,00	4,00
Mg#	83,9	82,4	84,6	75,1	75,2	84,6	74,4	74,0	69,3	80,8	76,2	77,6	71,0	81,0	80,6
Wo	**46,3**	**46,8**	**45,6**	**40,1**	**41,3**	**44,1**	**41,2**	**48,5**	**48,5**	**46,8**	**48,8**	**47,8**	**50,6**	**47,9**	**42,4**
En	**44,3**	**42,8**	**45,0**	**43,4**	**42,4**	**46,3**	**42,2**	**36,8**	**34,3**	**41,9**	**37,8**	**39,4**	**33,8**	**41,2**	**45,3**
Fs	**9,5**	**10,4**	**9,3**	**16,5**	**16,3**	**9,6**	**16,6**	**14,7**	**17,2**	**11,3**	**13,4**	**12,8**	**15,6**	**10,9**	**12,4**

Table 3. Selected microprobe analyses for orthopyroxene from quartz andesites (Oaş-Gutâi Mts.). Structural formulas are calculated on the basis of 6O, according to Cawthorn & Collerson (1974). Fe_{TOTAL} as Fe^{2+}.

Sample	7568-M				7571-M					
Point	19	20	21	22	13	14	15	16	17	18
SiO_2	53,34	53,35	52,95	53,07	53,38	53,19	53,76	53,11	51,25	52,75
TiO_2	0,25	0,25	0,10	0,11	0,13	0,07	0,15	0,15	0,16	0,14
Al_2O_3	2,77	2,65	0,50	0,51	0,51	0,47	0,59	0,74	1,09	0,71
FeO	17,14	16,99	25,33	25,08	26,91	26,29	23,28	23,99	23,47	22,93
MnO	0,54	0,54	0,98	1,03	1,28	1,19	0,84	0,91	0,96	0,84
MgO	24,75	24,67	19,08	19,23	18,07	18,65	20,83	19,78	22,04	20,82
CaO	1,43	1,36	0,96	0,94	0,78	0,84	1,09	1,06	1,32	1,23
Na_2O	0,04	0,01	0,02	0,07	0,03	0,02	0,01	0,02	0,04	0,02
NiO	0,00	0,00	0,00	0,00	0,00	0,00	0,01	0,00	0,00	0,00
Cr_2O_3	0,03	0,02	0,03	0,00	0,00	0,00	0,00	0,00	0,00	0,02
Total	100,29	99,84	99,96	100,05	101,09	100,72	100,56	99,75	100,34	99,45
Si	1,94	1,95	2,01	2,01	2,02	2,02	2,01	2,01	1,91	1,99
Al^{IV}	0,06	0,05	0,00	0,00	0,00	0,00	0,00	0,00	0,05	0,01
Al^{VI}	0,06	0,06	0,02	0,02	0,02	0,02	0,03	0,03	0,00	0,02
Ti	0,01	0,01	0,00	0,00	0,00	0,00	0,00	0,00	0,00	0,00
Fe^{2+}	0,52	0,52	0,81	0,80	0,85	0,83	0,73	0,76	0,73	0,72
Mn	0,02	0,02	0,03	0,03	0,04	0,04	0,03	0,03	0,03	0,03
Mg	1,34	1,34	1,08	1,09	1,02	1,05	1,16	1,12	1,22	1,17
Ca	0,06	0,05	0,04	0,04	0,03	0,03	0,04	0,04	0,05	0,05
Na	0,00	0,00	0,00	0,01	0,00	0,00	0,00	0,00	0,00	0,00
Ni	0,00	0,00	0,00	0,00	0,00	0,00	0,00	0,00	0,00	0,00
Cr	0,00	0,00	0,00	0,00	0,00	0,00	0,00	0,00	0,00	0,00
Total cations	4,00	4,00	4,00	4,00	4,00	4,00	4,00	4,00	4,00	4,00
Mg#	74,1	74,2	59,9	60,3	57,1	58,4	63,9	62,0	65,0	64,3
Wo	**2,9**	**2,8**	**2,0**	**2,0**	**1,6**	**1,7**	**2,2**	**2,2**	**2,6**	**2,5**
En	**69,3**	**69,5**	**55,2**	**55,6**	**52,4**	**53,8**	**59,3**	**57,3**	**60,1**	**59,4**
Fs	**27,8**	**27,7**	**42,8**	**42,4**	**45,9**	**44,5**	**38,5**	**40,5**	**37,4**	**38,1**

5.3. Amphiboles

The amphiboles are well represented both quantitatively (until 6-8% of the weight of the rock), and as sizes (max. 10 mm). They are as prismatic, elongated, rarely fresh phenocrysts, frequently being substituted by the assemblege clinopyroxenes, plagioclase feldpars and opaque minerals („breakdown" amphiboles, Nixon, 1988) or they show marginal fine opacitic rims. Sometimes they contain inclusions of small prismatic plagioclase feldspars and granular pyroxenes, Ti-magnetite and ilmenite inclusions (Fig. 5.7b).

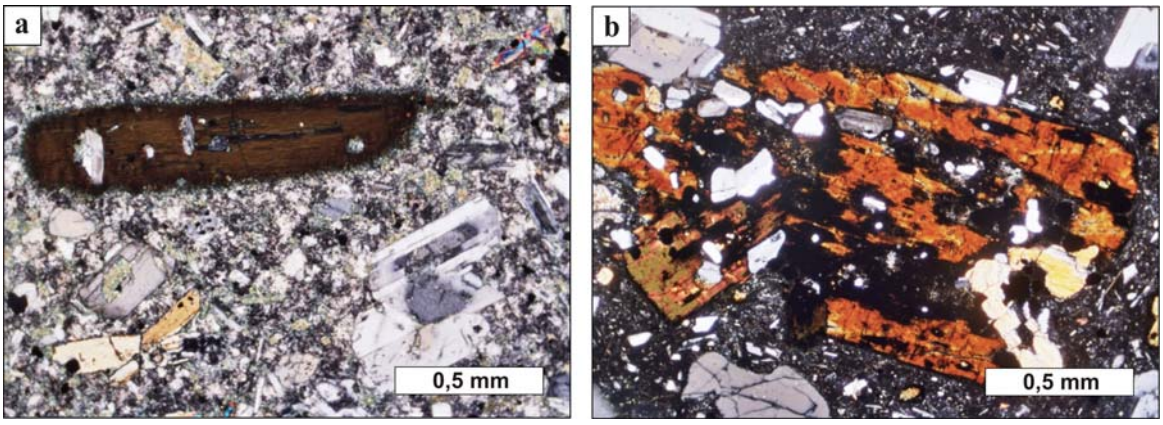

Fig. 5.7. Microphotographs of amphibole phenocrysts from the quartz andesites. a) Amphibole phenocryst with opacitic rim (Sample 7605-M); b) Amphibole phenocryst with feldspar, pyroxene and opaque minerals inclusions (Sample 7670-M). P+.

The amphiboles from the quartz andesites are exclusively calcic amphiboles (according to the IMA classification; Leake *et al.* 1997), with $(Ca+Na)_B \geq 1.00$, $Na_B < 0.50$ and $Ca_B > 1$ (Fig. 5.8a), most of them being magnesio-hornblende (Fig. 5.8b). On the whole the contents of the main oxides varies in the following intervals: SiO_2=42.3-51.4%, Al_2O_3=6.5-10.2%, FeO=14.2-17.3%, MgO=10.3-13.3%, and the magnesium number (Mg#) has values between 56.4 and 64.9. Within the same amphibole crystal the chemical composition is relatively constant, the variation interval of the above mentioned oxides is around 1% (Fig. 5.9a,b; table 4). The magnesium number (Mg#) also varies within a small interval, between 56.4 and 64.9.

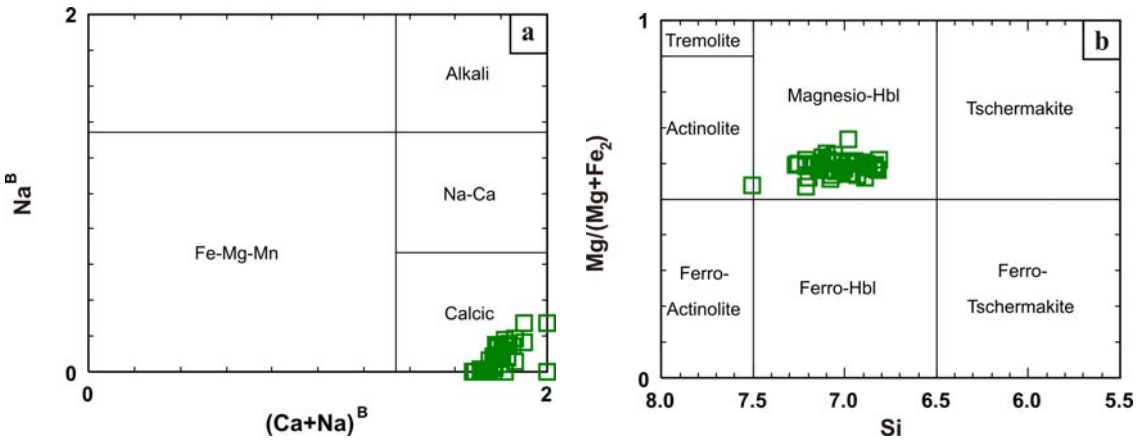

Fig. 5.8. Plotting of the amphibole electrone microprobe data in the IMA classification diagrams (Leake *et al.* 1997).

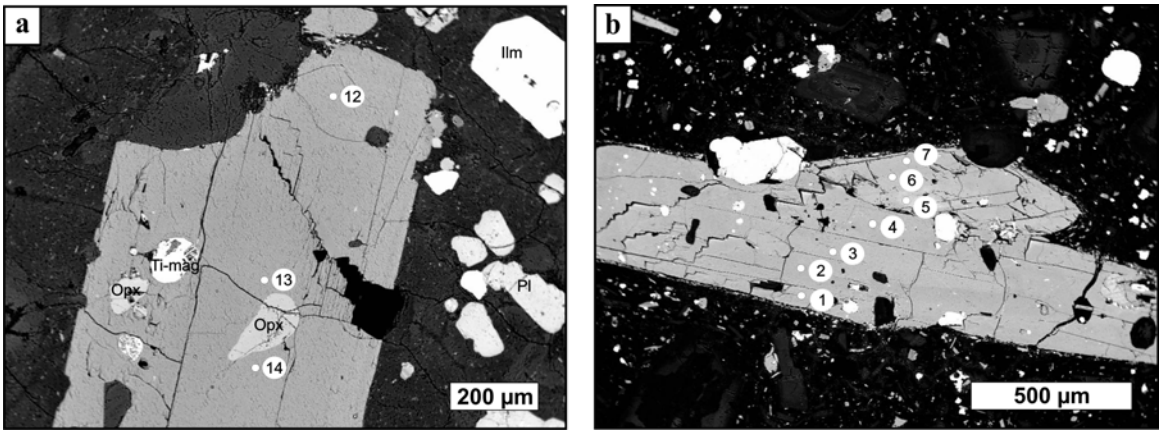

Fig. 5.9. BSE images of amphiboles from the quartz andesites. a) Subhedral phenocryst with orthopyroxene and Ti-magnetite inclusions (Sample 7560-M); b) Twinned euhedral phenocryst .(Sample 7571-M, microanalysis points 1-7); Abbreviations: Opx for orthopyroxenes, Ti-mag for Ti-magnetite, Pl for plagioclase, Ilm for ilmenite.

Table 4. Selected microprobe analyses for amphibole from quartz andesites (Oaş-Gutâi Mts.). Structural formulas are calculated on the basis of 23O, according to Richard & Clarke (1990). Fe_{TOTAL} as Fe^{2+}.

Sample	7560-M			7571-M						
Point	12	13	14	1	2	3	4	5	6	7
SiO_2	50.91	49.44	50.27	45.24	46.84	45.32	45.26	42.32	45.32	45.30
TiO_2	1.60	1.72	1.79	1.74	1.52	1.64	1.43	2.19	1.66	1.47
Al_2O_3	7.14	7.88	7.99	7.88	6.93	7.83	7.74	10.21	7.53	7.57
FeO	14.95	14.34	14.25	15.88	15.64	16.24	16.12	17.26	16.10	15.94
MnO	0.30	0.22	0.20	0.35	0.31	0.37	0.34	0.30	0.32	0.28
MgO	13.07	13.36	13.35	12.45	13.39	12.65	12.68	11.28	12.78	12.99
CaO	11.00	11.12	11.07	10.83	10.86	10.84	10.79	10.91	10.95	11.01
Na_2O	1.29	1.44	1.44	1.21	1.18	1.34	1.30	1.59	1.22	1.21
K_2O	0.32	0.39	0.39	0.45	0.26	0.43	0.41	0.54	0.43	0.42
Cr_2O_3	0.00	0.00	0.00	0.01	0.00	0.00	0.00	0.00	0.02	0.00
Total	100.56	99.90	100.73	96.05	96.94	96.66	96.06	96.60	96.33	96.17
TSi	7.21	7.06	7.10	6.83	6.97	6.82	6.84	6.44	6.84	6.84
TAl	0.79	0.94	0.90	1.17	1.03	1.18	1.16	1.56	1.16	1.16
TTi	0.00	0.00	0.00	0.00	0.00	0.00	0.00	0.00	0.00	0.00
Sum T	8.00	8.00	8.00	8.00	8.00	8.00	8.00	8.00	8.00	8.00
CAl	0.41	0.39	0.43	0.24	0.19	0.20	0.22	0.27	0.17	0.18
CTi	0.17	0.18	0.19	0.20	0.17	0.19	0.16	0.25	0.19	0.17
CCr	0.00	0.000	0.00	0.00	0.000	0.00	0.00	0.00	0.00	0.00
CMg	2.76	2.84	2.81	2.80	2.97	2.84	2.86	2.56	2.88	2.92
CFe 2	1.66	1.59	1.57	1.76	1.67	1.77	1.76	1.92	1.76	1.73
CMn	0.00	0.00	0.00	0.00	0.00	0.00	0.00	0.00	0.00	0.00
Sum C	5.00	5.00	5.00	5.00	5.00	5.00	5.00	5.00	5.00	5.00
BMg	0.00	0.00	0.00	0.00	0.00	0.00	0.00	0.00	0.00	0.00
BFe 2	0.11	0.13	0.11	0.25	0.28	0.27	0.28	0.28	0.27	0.29
BMn	0.03	0.03	0.02	0.04	0.04	0.05	0.04	0.04	0.04	0.03
BCa	1.67	1.70	1.68	1.71	1.68	1.68	1.68	1.68	1.69	1.68
BNa	0.19	0.14	0.19	0.00	0.00	0.00	0.00	0.00	0.00	0.00
Sum B	2.00	2.00	2.00	2.00	2.00	2.00	2.00	2.00	2.00	2.00
ACa	0.00	0.00	0.000	0.04	0.05	0.07	0.07	0.10	0.08	0.10
ANa	0.17	0.25	0.21	0.36	0.34	0.39	0.38	0.47	0.36	0.35
AK	0.06	0.07	0.07	0.09	0.05	0.08	0.08	0.11	0.08	0.08
Sum A	0.23	0.32	0.28	0.49	0.44	0.54	0.53	0.68	0.52	0.53
Sum cat	15.23	15.32	15.28	15.49	15.44	15.54	15.53	15.68	15.52	15.53
Mg #	63.4	64.9	65.0	60.8	62.9	60.7	60.9	56.4	61.1	61.7

5.4. Quartz

The quartz phenocrysts are present in various proportions (1.0-6.5%) and has various sizes (0.2-6.0 mm). Generally, the quartz crystals have subhedral and anhedral outlines, often rounded (Fig. 5.10a), showing in most of the cases cracks that result in a characteristic aspect of the crystals. They are frequently corroded (Fig. 5.11a), sometimes with skeletal aspect (Fig. 5.10b, Fig. 5.11b).

In the basic quartz andesites, pyroxene coronas can be noticed around the quartz crystals, suggesting the existence of magma mixing processes (Clynne, 1999).

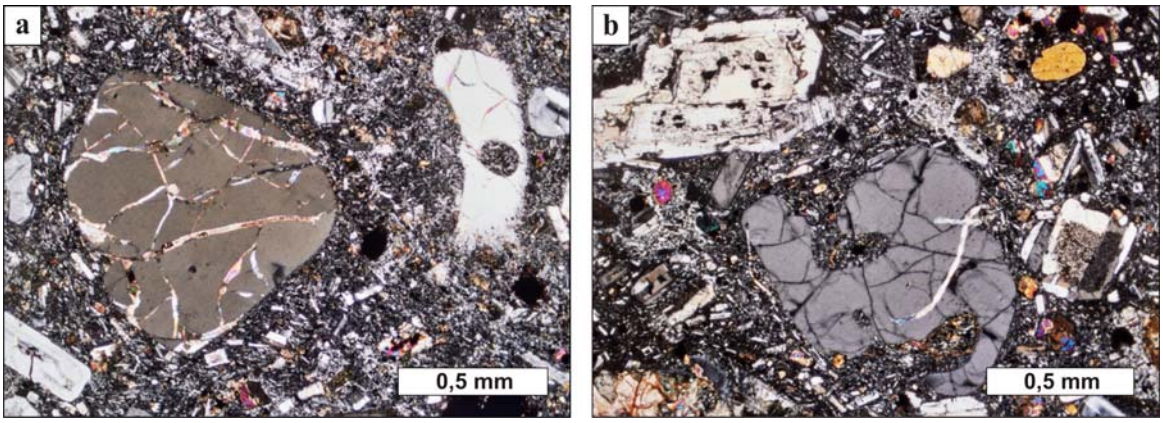

Fig. 5.10. Microphotographs of quartz phenocrysts from the quartz andesites. a) Quartz phenocryst with subrounded outline (Sample 7566-M); b) Intensely corroded quartz phenocryst, with skeletal aspect (Sample 7565-M). P+.

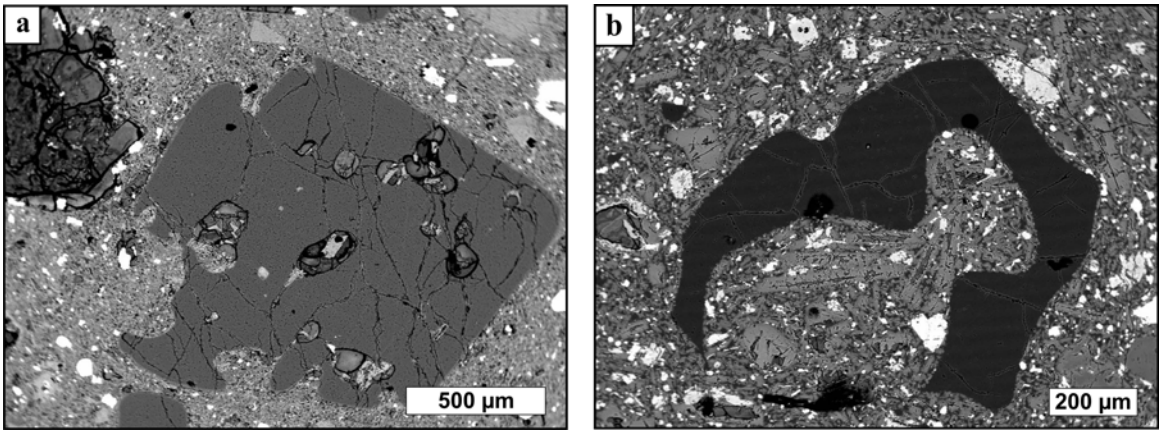

F**ig. 5.11.** BSE images of quartz phenocrysts. a) Subhedral phenocryst with resorpsion zones and deposits of secondary minerals (clorites) (Sample 7554-M); d) Phenocryst strongly corroded with skeletal aspect (Sample 7568-M).

5.5 Accessory minerals

The iron and titanium oxides, that is titanomagnetite and ilmenite, are the commonest opaque accessory minerals in the quartz andesites. They appear as isolated grains or associated with orthopyroxene, clinopyroxene and plagioclase phenocrysts in the groundmass (Fig. 5.12a). The Fe and Ti oxides also appear as fine inclusions in the plagioclase feldspar, pyroxene and amphibole phenocrysts (Fig. 5.12b). Their chemical composition is shown in table 5.

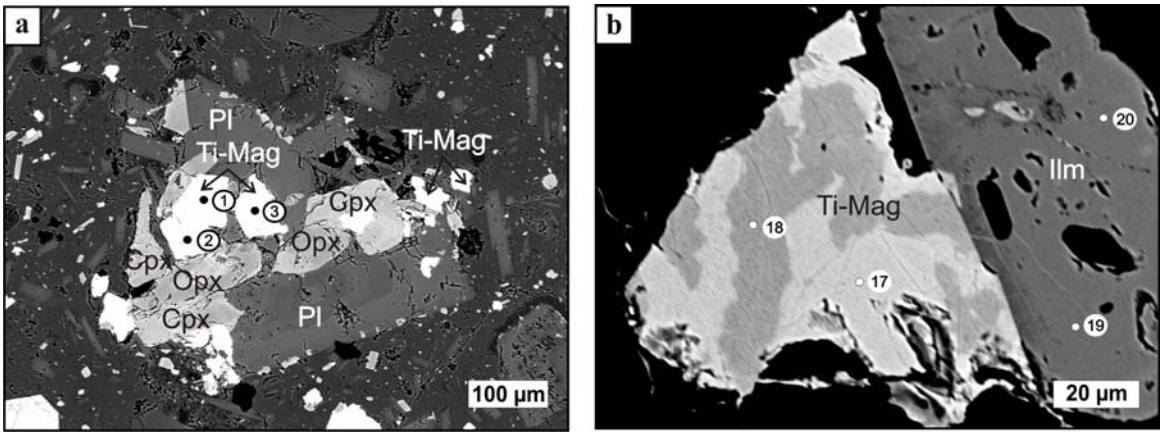

Fig. 5.12 BSE images of Ti-magnetite and ilmenite. a) Cluster of plagioclase feldspar (Pl), orthopyroxene (Opx), clinopyroxene (Cpx) and titanomagnetite (Ti-Mag) (Sample 7571-M, microanalysis points 1-3); b) Titanomagnetite (Ti-Mag) and ilmenite (Ilm) inclusions in orthopyroxenes (Sample 7566-M, microanalysis points 17-20).

Table 5. Selected microprobe analyses for Ti-magnetite and ilmenite from quartz andesites (Oaş-Gutâi Mts.). Abbreviation: nd-not determined.

Mineral	Ti-magnetite					Ilmenite	
Sample	**7566-M**		**7571-M**			**7566-M**	
Point	17	18	1	2	3	20	19
SiO_2	0.03	0.20	0.41	0.09	0.10	0.00	0.07
TiO_2	7.44	7.56	9.74	9.84	9.55	46.85	45.43
Al_2O_3	1.11	1.03	3.66	3.89	3.67	0.03	0.01
FeO	83.98	79.95	75.74	75.65	76.60	50.86	51.44
Cr_2O_3	0.06	0.05	0.11	0.10	0.11	0.01	0.02
MnO	0.21	0.07	0.35	0.35	0.35	0.58	0.73
NiO	nd	nd	1.37	1.52	2.08	nd	nd
MgO	0.42	0.20	0.06	0.02	0.03	1.09	1.59
BaO	0.00	0.05	nd	nd	nd	0.31	0.37
CaO	0.06	0.17	0.00	0.00	0.05	0.09	0.26
Na_2O	0.05	0.00	0.00	0.00	0.00	0.00	0.00
K_2O	0.00	0.00	0.00	0.00	0.00	0.00	0.00
Total	93.84	91.27	93.82	94.02	92.20	99.80	99.92

5.6. Secondary minerals

The plagioclase feldspars, orthopyroxenes, clinopyroxenes and amphiboles from the quartz andesites are generally fresh, but sometimes they are partly or totally replaced by secondary minerals, like carbonates, illite, chlorite, smectite etc.

Thus, some of the plagioclase phenocrysts are partly replaced by phyllosilicates of the illite group, with a K_2O content higher than 9% (Fig. 5.13a; table 6 – sample 7566-M). Other plagioclase phenocrysts core are replaced by Fe carbonates (siderite) with a low content of Mg and Ca, asociated with interstratified minerals of the chlorite and smectite groups (Fig. 5.13b; table 6 – sample 7554-M). Pyroxene phenocrysts (orthopyroxenes and clinopyroxenes) are mainly replaced by minerals of the chlorite and smectite groups (Fig. 5.13c,d; table 6 – samples 7567-M and 7559-M). The FeO in these minerals varies between 18-25%, and the MgO content varies between 14 and 17%.

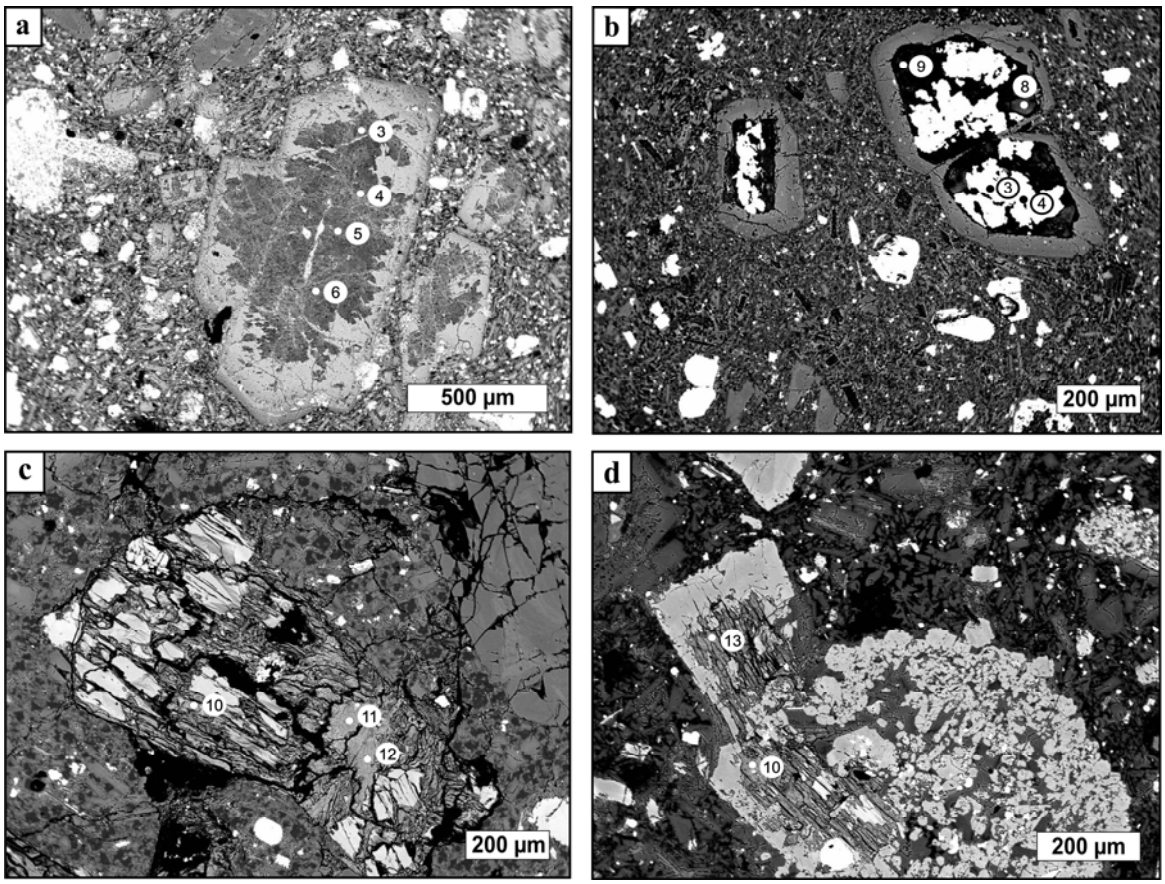

Fig. 5.13. BSE images of secondary minerals. a) Plagioclase feldspar phenocryst replaced in the central zone by illite (Sample 7566-M); b) Plagioclase phenocryst replaced by carbonates and chlorite (Sample 7554-M); c) Orthopyroxene phenocryst partly replaced by chlorite (sample 7567-M); d) Clinopyroxene phenocrysts with secondary minerals from the chlorite group (sample 7559-M).

Table 6. Selected microprobe analyses for secondary minerals from quartz andesites (Oaş-Gutâi Mts.). Abbreviation: nd-not determined.

Proba	**7566-M**				**7554-M**				**7567-M**			**7559-M**	
Punct de analiză	3	4	5	6	3	4	8	9	10	11	12	10	13
SiO_2	46.11	44.92	46.28	46.51	0.00	0.03	46.52	46.66	44.69	42.47	44.59	33.85	34.99
TiO_2	0.00	0.04	0.03	0.00	0.00	0.01	0.00	0.00	0.07	0.15	0.03	0.01	0.00
Al_2O_3	33.24	33.97	34.11	34.56	0.04	0.00	9.80	10.79	7.15	7.71	7.25	10.96	10.92
FeO	2.67	2.76	1.61	2.17	48.15	46.32	14.03	12.15	18.85	19.84	18.86	25.06	23.70
Cr_2O_3	0.02	0.00	0.00	0.00	0.01	0.02	0.00	0.03	0.03	0.02	0.00	0.04	0.00
MnO	0.06	0.00	0.04	0.01	1.75	0.77	0.22	0.14	0.10	0.07	0.08	0.27	0.27
NiO	nd	nd	nd	nd	0.04	0.02	0.00	0.01	nd	nd	nd	nd	nd
MgO	1.26	1.12	0.89	0.68	4.07	2.71	6.37	5.07	14.21	15.01	15.25	16.96	17.34
BaO	0.05	0.07	0.08	0.07	nd	nd	nd	nd	0.03	0.00	0.00	0.00	0.00
CaO	0.20	0.37	0.24	0.13	2.99	6.98	0.83	0.73	1.38	1.36	1.70	0.40	0.63
Na_2O	0.19	0.26	0.21	0.14	0.01	0.01	0.49	0.51	0.45	0.60	0.69	0.07	0.14
K_2O	9.00	9.08	9.32	9.68	0.00	0.00	0.29	0.28	0.09	0.06	0.07	0.00	0.00
Total	92.80	92.58	92.80	93.95	57.04	56.86	78.54	76.38	87.05	87.28	88.51	87.62	87.99

5.7. Groundmass

The groundmass of the quartz andesites shows different degrees of crystallinity, from hyalopillitic (Fig. 5.14a) to intersertal (Fig. 5.14b), and even holocrystalline. The hyalopillitic groundmass, which contains plagioclase feldspar microlites with tabular or elongated prismatic shape, shows different textural aspects, from those with a slight orientation around the phenocrysts to the fluidal ones (Fig. 5.15a). Sometimes, beside the plagioclase are also present granular pyroxenes. In some cases, the incipient devitrification phenomenon of the glassy groundmass is noticed, together with the formation of some areas with spherulitic texture (Fig. 5.15b).

The chemical composition of the groundmass is presented in table 7. To be noticed the high SiO_2 contents (between 64.5 and 86.1%) together with Al_2O_3 contents that vary within a large interval (between 6.4 and 18.4%). CaO and Na_2O are also present in lower proportions. Also to be noticed the variation of the K_2O content, which in some analysed points is zero, and in others shows high values (till 11.5%) due to the presence of the secondary minerals (clay minerals).

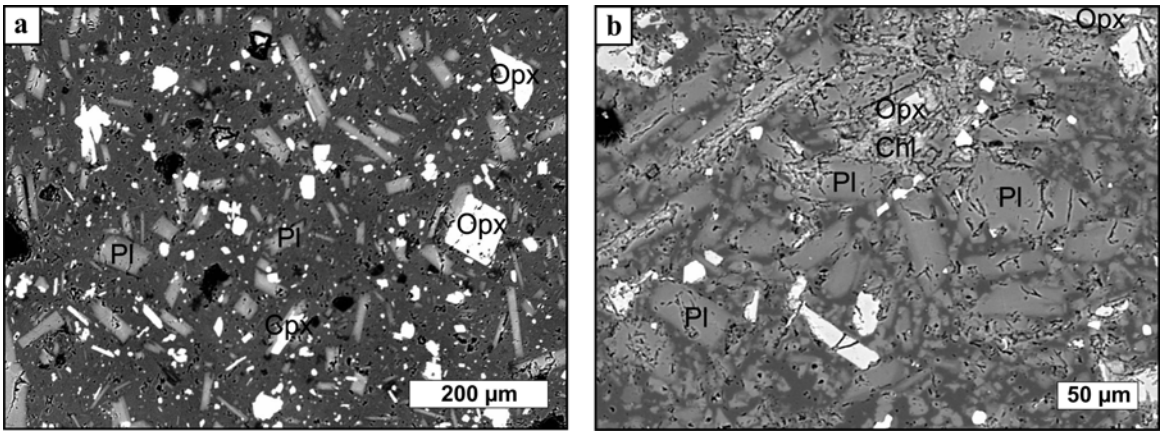

Fig. 5.14. BSE images of the groundmass. a) Hyalopillitic texture, with rare plagioclase feldspar (Pl), orthopyroxene (Ppx) and clinopyroxene (Cpx) microlites in a glassy groundmass; b) Intersertal texture, with plagioclase feldspar (Pl) and orthopyroxene (Opx) microlites and secondary minerals-chlorite (Chl)

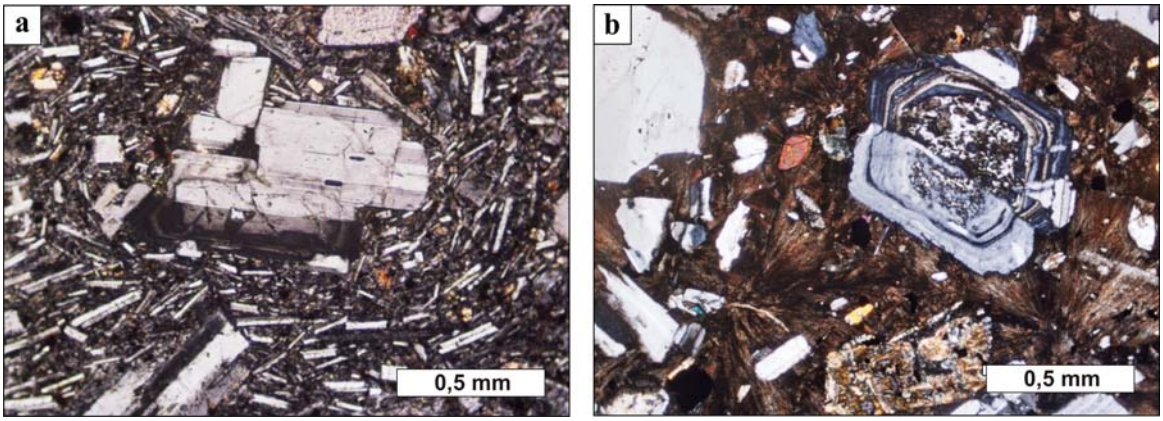

Fig. 5.15 Microphotographs of the groundmass of the quartz andesites. a) Plagioclase phenocrysts in a groundmass with oriented fluidal texture (Sample 7645-M); b) Twinned and zoned plagioclase phenocryst in groundmass with spherulitic texture (Sample 560-M). P+.

Table 7. Selected microprobe analyses for the groundmass from quartz andesites (Oaş-Gutâi Mts.). Abbreviation: nd-not determined.

Proba	**7554-M**		**7559-M**	**7565-M**	**7567-M**	**7571-M**				
Punct de analiză	15	16	10	15	23	3	5	14	22	23
SiO_2	86.09	72.09	64.48	84.89	66.75	79.67	76.38	79.38	77.29	79.39
TiO_2	0.09	0.07	0.10	0.19	0.04	0.31	0.25	0.35	0.28	0.36
Al_2O_3	6.43	16.87	18.00	7.46	18.40	10.69	12.20	9.97	11.00	9.98
FeO	0.30	0.24	0.51	0.45	0.50	0.89	2.54	1.03	0.96	1.00
Cr_2O_3	0.03	0.00	0.00	0.00	0.01	0.04	0.01	0.00	0.02	0.00
MnO	0.00	0.00	0.00	0.01	0.00	0.00	0.05	0.00	0.05	0.00
NiO	0.00	0.03	nd	nd	nd	0.00	0.68	0.05	0.01	0.03
MgO	0.08	0.02	0.05	0.10	0.10	0.04	1.53	0.89	0.06	0.03
BaO	nd	nd	0.13	0.05	0.15	nd	nd	nd	nd	nd
CaO	1.19	2.98	0.63	0.44	2.27	0.69	2.32	1.22	0.72	0.40
Na_2O	2.18	4.57	2.78	1.33	4.74	1.00	4.39	5.46	1.77	1.23
K_2O	1.13	3.67	11.59	4.26	6.58	4.31	0.00	0.00	5.02	5.36
Total	97.53	100.52	98.26	99.16	99.54	97.63	100.34	98.34	97.18	97.77

CH. 6. GEOCHEMISTRY OF THE PANNONIAN QUARTZ ANDESITES FROM THE OAŞ-GUTÂI MTS.

The geochemistry of the quartz andesites is based on major, minor, and rare earths elements analysis made on 26 representative samples from the Gutâi and Oaş Mts.

6.1. Major elements chemistry

Major elements data of the quartz andesites from Oaş-Gutâi mountains are reported in table 8. Two groups were separated in the quartz andesites from Gutâi on the basis of SiO_2 content: „basic" quartz andesites with SiO_2 ranging from 56.33 to 58.54 wt % and „acidic" quartz andesites with SiO_2 content between 59.19 şi 63.49 wt %. The quartz andesites from Oaş mountains are very homogeneous with SiO_2 ranging from 61.05 to 61.55wt %.

The quartz andesites from Oaş-Gutâi mountains are predominantly andesites according to the TAS diagram (LeBas *et al*., 1986). Some of the samples from the „basic" quartz andesites group from Gutâi plott in the basaltic andesite field and one of the „acidic" quartz andesites plotts in the field of dacite (Fig. 6.1a). They are calc-alkaline rocks, typically medium-K volcanics according to the K_2O - SiO_2 diagram (Gill, 1981, Fig. 6.1b).

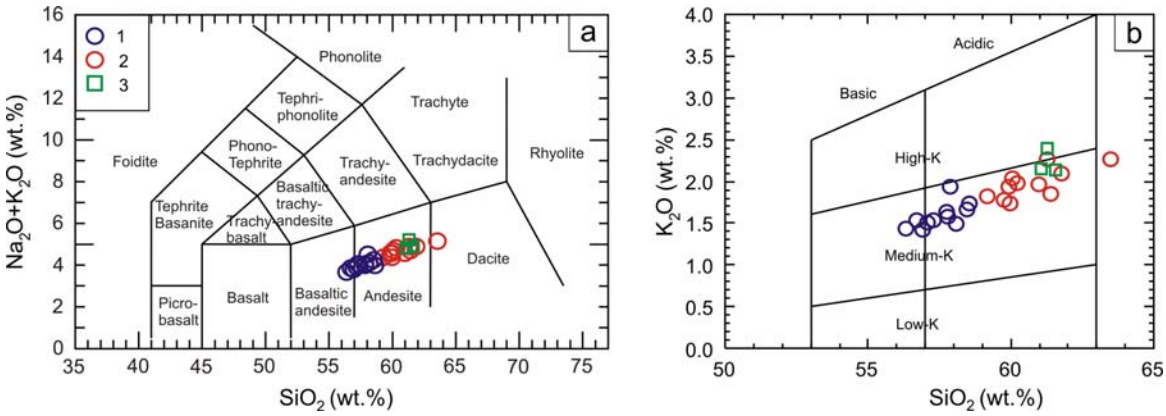

Fig. 6.1. Plott of the chemical data for quartz andesites from Oaş-Gutâi Mts. into: a). the TAS diagram (LeBas et al., 1986); b) the SiO_2 vs. K_2O discrimination diagram of Gill (1981). Symbols: 1. „Basic" quartz andesites from Gutâi Mts.; 2. „Acidic" quartz andesites from Gutâi Mts.; 3. Quartz andesites from Oaş Mts.

Table 8. Whole rock chemistry for quartz andesites samples (major elements in wt.%; minor, trace and RE elements in ppm).

Sample	7551-M	7552-M	7553-M	7554-M	7555-M	7556-M	7557-M	7558-M	7559-M	7560-M	7561-M	7562-M	7563-M
Area (Mts.)	Gutâi	Gutâi	Gutâi	Gutâi	Gutâi	Gutâi	Gutâi	Gutâi	Gutâi	Gutâi	Gutâi	Gutâi	Gutâi
Locality	Poiana Cremenii	Cuţilor Valley	Şuior Valley	Milerii Valley	Hijii Valley	Firiza Valley	Roşie Valley	Polomestru Valley	Franţuşca Valley	Pleştioara Peak	Ostra Quarry	Tocastru Peak	Tocastru Valley
SiO_2	61.27	59.91	59.19	60.96	59.96	60.06	58.54	56.33	57.08	63.49	57.88	56.91	58.10
TiO_2	0.58	0.65	0.66	0.58	0.69	0.68	0.69	0.71	0.72	0.56	0.70	0.70	0.74
Al_2O_3	15.52	15.85	15.69	15.88	15.80	16.30	15.76	17.20	16.58	16.02	16.55	16.37	16.86
Fe_2O_3	5.94	6.50	6.80	7.09	6.91	6.89	7.10	7.67	7.51	5.43	7.00	8.22	7.52
MnO	0.13	0.11	0.10	0.13	0.13	0.13	0.11	0.13	0.13	0.11	0.14	0.15	0.17
MgO	2.18	2.94	3.08	1.85	3.19	2.82	4.18	3.60	3.89	1.94	3.37	3.93	3.46
CaO	4.98	6.58	6.33	4.52	6.94	6.04	7.17	7.36	8.20	5.40	6.61	8.17	7.32
Na_2O	2.64	2.63	2.57	2.65	2.68	2.69	2.26	2.26	2.43	2.92	2.56	2.37	2.62
K_2O	2.27	1.93	1.82	1.97	1.74	2.03	1.73	1.44	1.51	2.27	1.94	1.42	1.49
P_2O_5	0.11	0.11	0.10	0.12	0.12	0.12	0.13	0.11	0.10	0.10	0.12	0.11	0.12
LOI	4.20	2.70	3.50	4.10	1.70	2.10	2.10	3.00	1.70	1.60	3.00	1.50	1.40
Sum	99.87	99.86	99.86	99.88	99.86	99.85	99.82	99.83	99.84	99.88	99.84	99.85	99.85
#Mg	42.10	47.26	47.29	34.08	47.77	44.78	53.84	48.18	50.65	41.45	48.82	48.64	47.69
Ba	366	321	321	389	307	399	413	388	271	404	376	244	329
Sc	16	19	20	18	23	21	25	23	25	16	23	27	22
Cr	20.5	27.4	20.5	27.4	41.0	13.7	6.8	13.7	47.8	13.7	13.7	41.0	13.7
Mo	0.2	0.6	0.8	0.2	0.5	0.6	0.5	0.4	0.5	0.3	0.5	0.4	0.6
Cu	16.1	23.5	22.2	9.6	20.5	12.1	29.0	18.0	17.5	10.8	12.0	44.3	39.9
Pb	1.5	4.9	1.5	1.9	2.7	2.9	3.8	7.7	2.4	1.4	3.8	2.6	3.0
Zn	47	37	51	33	43	40	48	40	32	23	51	34	56
Ni	2.1	3.7	3.5	2.2	3.7	2.4	7.3	2.9	5.4	1.4	2.2	5.3	4.0
Co	11.8	15.4	17.1	10.0	16.3	16.0	20.4	19.0	21.2	12.6	16.2	24.4	19.4
Cs	2.0	1.3	1.6	4.1	1.6	2.8	2.3	12.4	10.6	3.2	1.7	1.9	4.2
Ga	14.6	16.1	16.4	15.5	15.4	16.3	16.7	16.3	16.4	16.0	17.2	16.3	17.8
Hf	2.9	2.6	2.8	3.0	2.9	3.0	3.0	2.5	2.6	2.8	3.5	2.1	2.5
Nb	7.3	7.6	7.0	7.7	6.2	8.1	6.6	6.1	6.5	7.3	7.5	6.1	6.5
Rb	69.8	62.2	59.6	61.7	53.2	73.3	54.3	50.6	47.9	74.5	62.4	47.0	47.4
Sn	1	1	1	2	1	2	2	1	1	1	1	1	2
Sr	201.1	227.3	234.6	207.0	248.5	234.1	259.1	252.7	278.4	214.9	235.2	251.2	250.1
Ta	0.6	0.6	0.6	0.6	0.5	0.5	0.5	0.5	0.5	0.7	0.6	0.4	0.5
Th	6.7	6.4	6.2	6.0	5.1	7.6	5.4	4.6	5.1	7.0	6.7	4.4	5.2
U	2.2	1.9	2.0	2.0	1.7	2.4	1.7	1.6	1.5	2.4	2.0	1.5	1.6
V	134	163	177	134	180	185	191	205	218	135	170	218	195
W	0.9	1.2	0.6	0.6	0.6	1.0	0.7	0.6	0.9	1.3	0.5	0.7	1.0
Zr	99.7	104.2	97.4	118.2	98.6	116.4	99.5	91.7	92.8	112.0	110.8	87.5	93.4
Y	24.3	20.2	19.4	23.8	18.8	25.1	18.5	20.1	20.9	19.7	23.2	19.4	21.4
La	17.1	15.3	15.5	18.5	13.9	19.1	15.3	13.7	13.1	16.9	18.6	12.0	14.1
Ce	32.1	33.2	33.2	38.0	30.1	41.2	33.2	30.4	28.9	35.3	40.0	26.5	30.9
Pr	3.82	3.67	3.73	4.40	3.45	4.77	3.73	3.43	3.29	3.80	4.58	3.09	3.51
Nd	14.2	15,0	15.0	17.6	14.2	18.9	13.9	13.5	14.3	14.9	18.1	12.3	13.4
Sm	3.22	3.17	3.37	3.68	3.04	4.15	3.41	3.16	3.21	3.02	3.87	2.92	3.25
Eu	0.85	0.80	0.83	1.00	0.84	0.99	0.86	0.87	0.86	0.83	0.99	0.86	0.89
Gd	3.07	3.17	3.18	3.84	3.03	4.23	3.31	3.53	3.40	3.33	3.88	3.24	3.44
Tb	0.57	0.56	0.56	0.65	0.54	0.74	0.55	0.59	0.59	0.54	0.68	0.56	0.61
Dy	3.16	3.09	3.21	3.71	3.16	3.94	3.06	3.34	3.53	3.24	3.91	3.18	3.47
Ho	0.72	0.70	0.66	0.81	0.68	0.86	0.64	0.70	0.74	0.68	0.84	0.70	0.73
Er	2.23	2.11	2.06	2.30	1.98	2.56	1.83	2.08	2.11	1.97	2.37	2.02	2.17
Tm	0.34	0.30	0.32	0.35	0.29	0.39	0.29	0.32	0.32	0.31	0.37	0.32	0.35
Yb	2.22	1.96	2.17	2.39	1.99	2.54	1.91	2.16	2.08	2.12	2.28	2.00	2.18
Lu	0.37	0.32	0.33	0.38	0.29	0.40	0.30	0.32	0.34	0.34	0.36	0.32	0.35

Mg#=100×MgO/(MgO+FeO_{TOT}). Fe_{TOT} as Fe_2O_3.

Table 1. Continued.

Sample	7564-M	7565-M	7566-M	7567-M	7568-M	7569-M	7570-M	7571-M	7572-M	7573-M	7574-M	7575-M
Area (Mts.)	Gutâi	Gutâi	Gutâi	Gutâi	Gutâi	Gutâi	Gutâi	Gutâi	Gutâi	Oaş	Oaş	Oaş
Locality	Runcu	Băiţa	Romlaş	Ulmoasa	Nopţii	Cioncaş	P. Tisei	Ouţului	Brada	Custurii	Târşolţ	Verdeş
	Peak	Valley	Valley	Peak	Valley	Valley	Peak	Valley	Valley	Valley	Valley	Valley
SiO_2	58.46	57.28	56.69	57.75	57.78	59.75	61.40	61.78	60.21	61.29	61.05	61.55
TiO_2	0.73	0.74	0.76	0.70	0.70	0.71	0.65	0.60	0.63	0.62	0.67	0.65
Al_2O_3	16.92	16.79	16.43	16.93	16.86	16.12	16.67	15.98	15.60	15.86	15.75	16.13
Fe_2O_3	7.57	7.55	7.53	7.07	7.74	6.69	6.39	5.90	6.74	5.77	6.09	5.97
MnO	0.15	0.13	0.14	0.14	0.15	0.17	0.13	0.12	0.12	0.11	0.14	0.11
MgO	3.05	3.59	3.55	3.08	3.52	2.14	2.21	2.76	2.34	2.08	2.16	2.17
CaO	7.03	7.68	8.59	7.07	7.32	6.48	6.13	6.15	5.70	5.39	5.72	5.57
Na_2O	2.62	2.56	2.32	2.44	2.43	2.84	2.84	2.83	2.86	2.83	2.69	2.77
K_2O	1.66	1.54	1.54	1.64	1.58	1.78	1.85	2.09	1.98	2.40	2.15	2.13
P_2O_5	0.13	0.12	0.10	0.13	0.11	0.12	0.13	0.10	0.15	0.14	0.17	0.16
LOI	1.50	1.90	2.20	2.90	1.70	3.10	1.50	1.60	3.50	3.30	3.30	2.60
Sum	99.85	99.85	99.86	99.86	99.85	99.88	99.88	99.86	99.85	99.83	99.84	99.83
#Mg	44.39	48.51	48.29	46.32	47.40	38.79	40.66	48.10	40.75	41.66	41.27	41.86
Ba	306	271	244	323	301	316	340	364	328	500	408	411
Sc	21	25	26	21	24	20	17	20	17	17	19	18
Cr	27.4	13.7	41.0	13.7	20.5	13.7	13.7	20.5	13.7	13.7	13.7	13.7
Mo	0.5	0.5	0.3	0.6	0.3	0.5	0.5	0.1	0.5	0.5	0.5	0.6
Cu	14.1	37.5	18.6	19.6	21.6	15.8	10.3	20.4	28.8	8.4	10.1	11.2
Pb	2.0	2.0	2.0	7.3	1.2	1.7	1.9	1.2	2.2	2.6	2.1	2.9
Zn	52	36	38	54	41	53	38	18	46	44	54	52
Ni	1.6	3.6	5.2	3.1	4.2	2.1	0.9	1.6	1.1	1.9	2.7	2.6
Co	18.8	20.3	20.7	16.4	20.4	14.3	14.4	16.6	13.0	10.7	10.8	10.9
Cs	1.8	3.5	3.6	1.3	2.1	2.3	2.4	5.0	1.9	2.9	1.8	2.4
Ga	17.7	17.0	16.0	18.2	17.0	17.4	16.6	15.3	16.3	16.9	15.3	16.3
Hf	2.9	2.2	2.4	2.8	2.9	2.3	2.9	2.9	3.1	3.7	4.2	4.3
Nb	7.1	5.7	5.9	6.9	6.2	6.5	7.9	6.8	7.3	9.0	8.3	8.9
Rb	52.9	49.9	50.1	53.9	53.0	58.3	59.9	69.3	63.6	88.6	79.5	76.9
Sn	1	1	1	1	1	1	1	1	1	1	2	1
Sr	275.2	263.7	248.4	239.4	232.4	240.3	244.9	247.5	222.1	233.3	233.4	237.1
Ta	0.5	0.5	0.5	0.5	0.5	0.5	0.6	0.5	0.5	0.7	0.6	0.6
Th	5.7	4.4	4.7	5.3	5.1	5.8	5.6	6.6	6.7	10.2	8.5	8.0
U	1.7	1.6	1.5	1.8	1.7	1.9	2.2	2.3	2.0	3.4	2.6	2.6
V	194	217	213	172	201	165	144	158	154	146	149	140
W	0.8	1.0	0.9	1.0	0.7	0.6	0.8	1.1	0.7	0.8	0.5	0.8
Zr	104.3	87.9	82.0	92.6	96.2	99.8	108.6	106.1	120.4	125.3	134.3	147.4
Y	21.2	20.0	19.6	20.2	20.1	19.3	22.2	18.9	22.0	21.0	24.2	22.8
La	14.8	12.4	12.1	15.3	14.2	14.8	16.6	17.1	17.1	20.4	19.4	19.4
Ce	32.9	27.9	27.1	34.7	32.4	31.8	37.5	35.5	36.6	41.9	42.1	42.2
Pr	3.73	3.19	3.10	3.78	3.57	3.49	4.03	3.76	4.27	4.74	4.76	4.80
Nd	15.0	13.2	13.0	14.5	13.9	13.8	16.5	14.4	17.0	16.7	16.6	19.1
Sm	3.48	3.06	2.99	3.44	3.38	3.09	3.59	3.11	3.76	3.66	3.85	3.91
Eu	0.96	0.90	0.86	0.91	0.86	0.88	0.91	0.81	0.94	0.90	0.97	1.02
Gd	3.63	3.38	3.31	3.59	3.40	3.21	3.72	3.23	3.68	3.39	3.72	3.71
Tb	0.62	0.58	0.58	0.61	0.60	0.56	0.63	0.55	0.63	0.58	0.67	0.64
Dy	3.66	3.37	3.39	3.35	3.57	3.28	3.52	3.31	3.78	3.77	3.95	3.75
Ho	0.77	0.74	0.69	0.75	0.70	0.69	0.75	0.66	0.74	0.71	0.77	0.76
Er	2.31	2.24	2.08	2.20	2.15	2.15	2.36	1.96	2.34	2.01	2.31	2.33
Tm	0.34	0.31	0.31	0.32	0.32	0.31	0.37	0.30	0.35	0.32	0.35	0.37
Yb	2.21	2.09	2.08	2.22	2.12	2.03	2.35	1.98	2.62	2.10	2.56	2.48
Lu	0.36	0.34	0.33	0.34	0.33	0.33	0.38	0.32	0.37	0.34	0.39	0.38

The compositional variation of the major elements in the quartz andesites from Oaş-Gutâi mountains as a function of wt % SiO_2 and MgO is illustrated in Figs. 6.2. TiO_2, Fe_2O_3, MgO show a negative correlation with SiO_2 , while the alkalies show a positive one (Fig.6.2a,b,c). In the same time, TiO_2, Fe_2O_3, and CaO show a positive correlation with MgO, in the case of the alkalies showing a negative one (Fig.6.2d,e,f). In both types of variation diagrams (reported both to SiO_2 and to MgO), the „basic" quartz andesites group from Gutâi is well individualised reported to the „acidic" quartz andesites group and to the quartz andesites from Oaş mountains (which both plott in the same field).

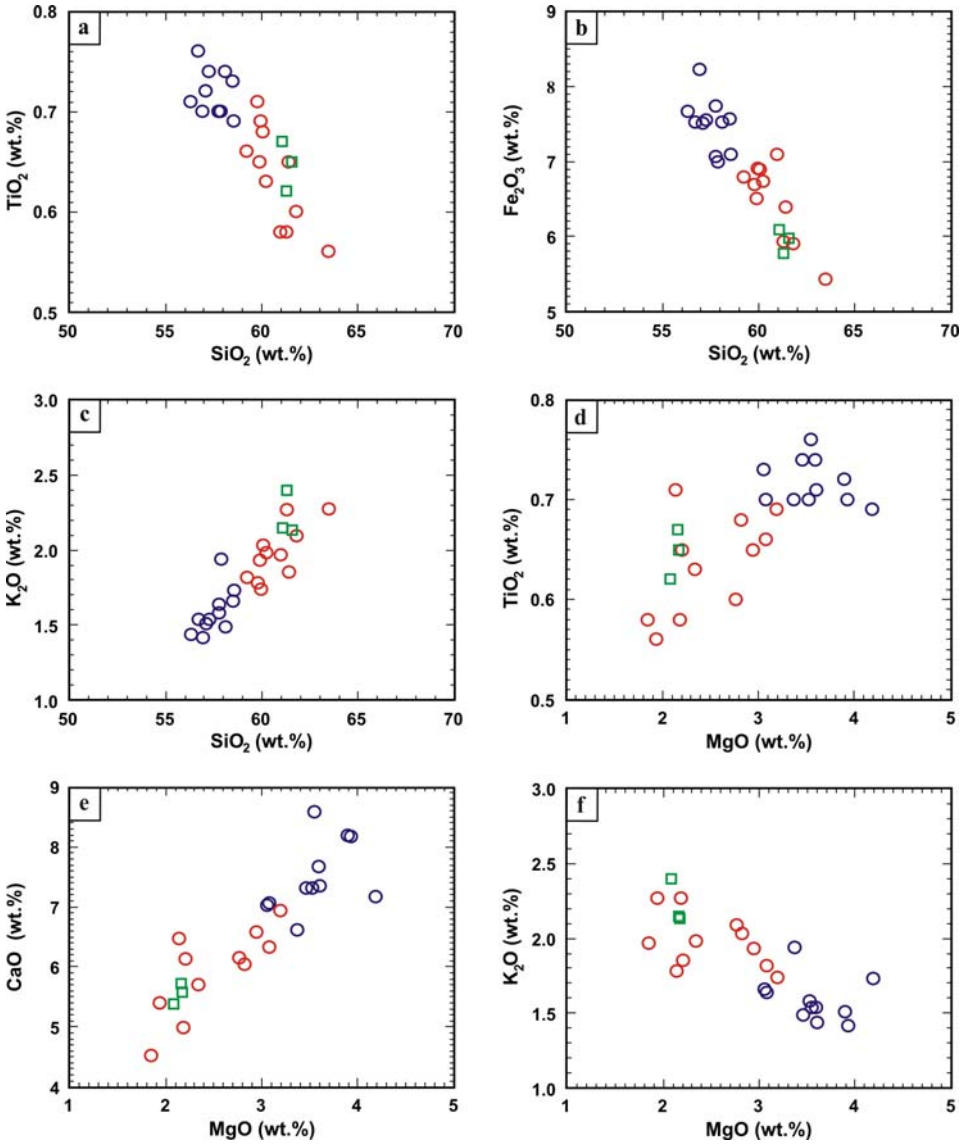

Fig. 6.2. Major elements vs. SiO_2 and MgO variation diagrams for the quartz andesites from Oaş-Gutâi Mts. Symbols as in Fig. 6.1a.

6.2. Minor elements geochemistry

The compatible trace elements (Ni, V) show a negative correlation with SiO_2 as a differentiation index (Fig. 6.3.a,b), while some crustal (Rb, Th) and source (Zr, Nb) incompatible trace elements show a clear positive correlation (Fig. 6.3c,d,e,f). In the last diagrams, the quartz andesites from Oaş mountains plott in a distinct field in the upper part of the variation domain. The „basic" quartz andesites group from Gutâi is also well individualised considering the variation of the Rb, Th and Zr, Nb respectively.

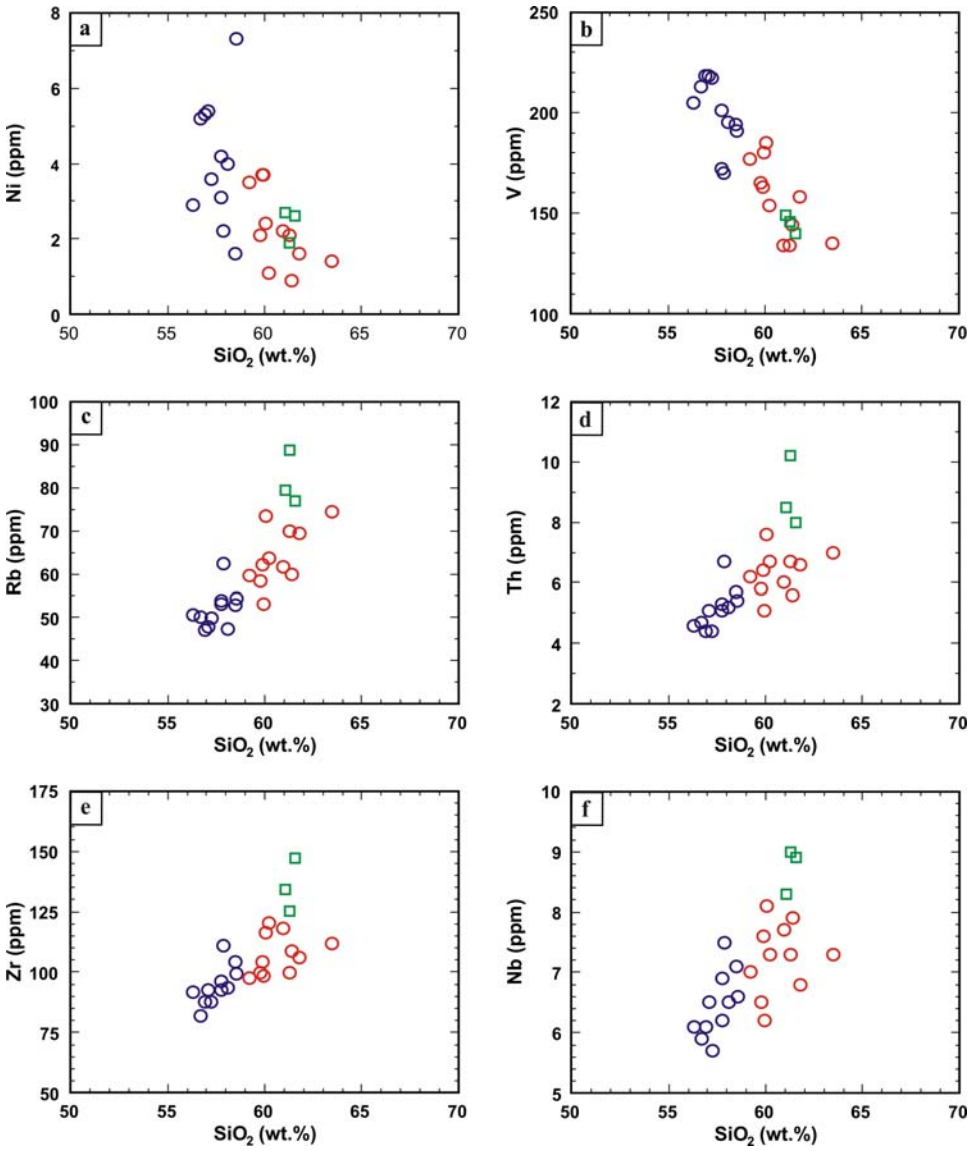

Fig. 6.3. Trace elements vs. SiO_2 variation diagrams for the quartz andesites from Oaş-Gutâi Mts. Symbols as in Fig. 6.1a.

6.3. Geochemistry of the rare earth elements (REE)

In the chondrite-normalized REE diagrams (Sun şi McDonough, 1989), both the „basic" and „acidic" quartz andesites from Gutâi Mts. (Fig. 6.4a) and the quartz andesites from Oaş Mts. (Fig. 6.4b), show quite similar patterns, with LREE enrichment and Eu negative anomalies, typical for volcanic rocks generated at the destructive margins/subduction zones (Wilson, 1989). These enrichments are slightly higher in the quartz andesites of the „acidic" group comparative with those of the „basic" group, as well as in the quartz andesites from Oaş.

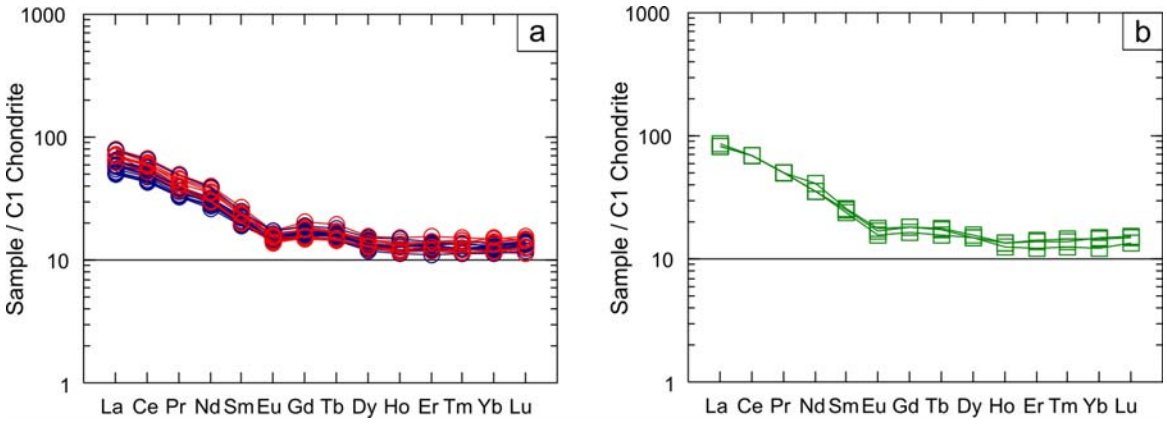

Fig. 6.4. Chondrite-normalized REE diagrams for the quartz andesites from: a). Gutâi Mts. ("acidic" and "basic" andesites group); b). Oaş Mts. Normalizing values are taken from Sun & McDonough (1989). Symbols as in Fig. 6.1a.

In the N-MORB normalized trace element diagrams (Fig. 9a,b) the quartz andesites from Oaş-Gutâi Mts. show enrichment of the LILE (Ba, Rb, Th, U, K) and LREE (La, Ce) and depletion of the HFSE (Nb, Ta) typical for volcanic rocks from subduction zones. The enrichment is higher in the case of the „acidic" quartz andesites group from Gutâi Mts comparative with those of „basic" quartz andesites group. The „basic"quartz andesites group have stronger Pb spike reported to „acidic" group and especially to the quartz andesites from Oaş Mts.

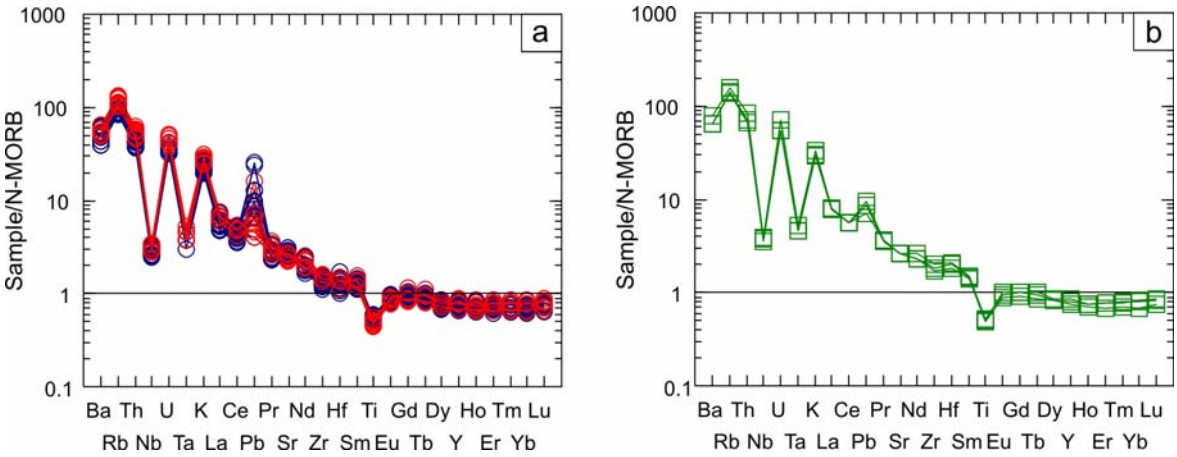

Fig. 6.5. N-MORB trace element normalized diagrams for the quartz andesites from: a) Gutâi Mts. (Group I and II); b) Oaş Mts. Normalizing values are taken from Sun & McDonough (1989). Symbols as in Fig. 6.1a.

6.4. Geochemical comparative considerations between the quartz andesites from the Oaş-Gutâi Mts. and other Pannonian volcanics from the Gutâi Mts.

The comparative study of the quartz andesites with the other Pannonian volcanics from the Oaş-Gutâi Mts. area (volcanics with which the quartz andesite are either in direct relationship or show a similar chemistry) emphasizes some similarities or dissimilarities regarding the behaviour of the minor elements and of the rare earth elements. In all cases, the similar patterns in the N-MORB normalized trace element diagrams can be noticed, with negative anomalies for Nb, Ta and Ti, and positive for Rb, U, K and Pb, respectivelly.

The values for the minor and for the rare earth elements are similar, with some slightly higher values for some of the elements in the case of some Pannonian volcanics in comparison with the quartz andesites.

CH. 7. THE PETROGENESIS OF THE PANNONIAN QUARTZ ANDESITES

The mineralogical study of the quartz andesites from the Oaş-Gutâi Mts., focused mainly on the chemistry of the minerals, as well as the geochemical study, based on major, minor and rare earth elements analysis emphasized a series of features typical for the igneous rocks generated in subduction zones: the calc-alkaline character, the significant enrichment in the lithofile elements (Ba, Rb, Sr, K, Pb, U, Th) and in the light rare earth elements (LREE), HFSE (Nb, Ta) depletion.

The generation of magma from the subduction zones takes place in the asthenospheric mantle situated above the subducting plate named „mantle wedge" (Gill, 1981). The nature of the source for the quartz andesites parental magma can be considered of NMORB type. The low U/Th ratios, the high Th contents (Fig. 7.1.) and the high values for the Th/Ce ratio of the quartz andesites from the Oaş-Gutâi Mts. suggest a low contribution of the fluids and a high contribution of the sediments from the subducted plate, respectively (according to Hawkesworth *et al.*, 1997). The higher involvement of the subducted sediments is also indicated by the Th/La variation versus Sm/La (Kimura and Yoshida, 2006).

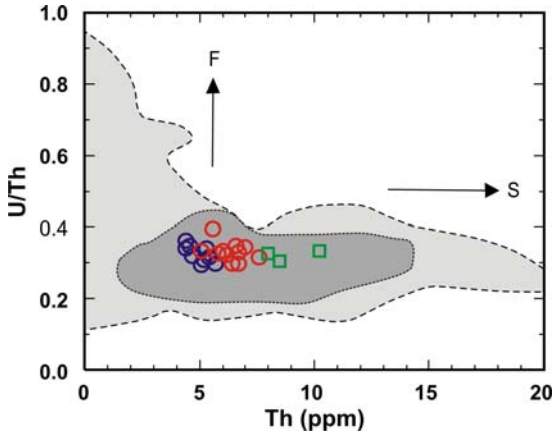

Fig. 7.1. U/Th vs. Th variation diagram for the quartz andesites from Oaş-Gutâi Mts. The dark grey field represent the Gutâi Mts. volcanics (from Kovacs, 2002) and the light grey field represent the worldwide active volcanic arcs (from Hawkesworth *et al,* 1997). F- fluids from the subducted slab variation trend; S – sediment components from the subducted slab variation trend; Symbols as in Fig. 6.1a.

A series of other processes that can be deciphered on the basis of the mineralogical and geochemical peculiarities are the processes that take place within the crustal magmatic chambers, mainly fractional crystallization, crustal assimilation and magma mixing.

The presence of fractional crystallization processes in the magmatic differentiation is constrainted by:

- Normal zoning of the plagioclase feldspars with decreases of the An content from 70-80% in the cores to 25-30% in the rims of the phenocrysts;

- The positive, respectively negative correlations, of the majore elements with the differentiation indexes (SiO_2 and MgO), as well as of the minor elements with the differentiation indexes(SiO_2 and Rb); the decrease of the TiO_2, Fe_2O_3, MgO and CaO contents with the increase of SiO_2 contents is due to the fractionation of the ferromagnesian minerals, especially of the pyroxenes, calcic plagioclases and of the Fe-Ti oxides, while the obvious decrease of the V content can be due to the intense fractionation of the pyroxenes;

- The positive correlation between Ba, La and Th on one side, and the Zr on the other side (Toothill *et al*., 2007) or the positive correlation between the Sm and La (Zelmer *et al*., 2003);

- The rare earth elements behavior in the chondrite-normalized diagrams and of the incompatible elements in the N-MORB normalized diagrams: the negative anomalies of Eu, that indicate plagioclase fractionation processes and the negative Ti anomalies, that indicate the strong fractionation of the Fe-Ti oxides (Ti-magnetite, ilmenite).

Informations regarding the involvment of the assimilation processes in the magmatic chambers from the upper crust, associated with the fractional crystallization (AFC type processes – De Paolo, 1981) are provided by:

- The increasing ratios between the incompatible crustal elements (K and Rb) and those characteristic for the source zones (Nb and Zr), due to the crustal assimilation; thus, the positive correlation between K/Nb or Rb/Nb and SiO_2, as well as between Rb/Nb and SiO_2, indicate crustal assimilations associated to the fractional crystallization;

- Typical assimilation - fractional crystallization (AFC) trends of the quartz andesites samples in some discriminant diagrams reporting different ratios (K_2O/Na_2O and Rb/Sr versus Rb/Zr, according to Hunter and Blake, 1995; Seghedi *et al.*, 2004; Fig. 7.2).

The presence of magma mixing processes within the crustal chambers are constrainted by minerals chemistry, especially of the plagioclase feldspars and pyroxenes, as well as by their textural aspects:

- The presence of the reverse zoning in the plagioclase feldspars and of the many recurence zones with large variations of the An content (30-35%) suggesting the modification of the magma composition by refilling of the magma chambers with hotter and

more basic melts and their mixing with the initial magma (Nelson and Montana, 1992; Singer *et al.,* 1995; Clynne,1999);

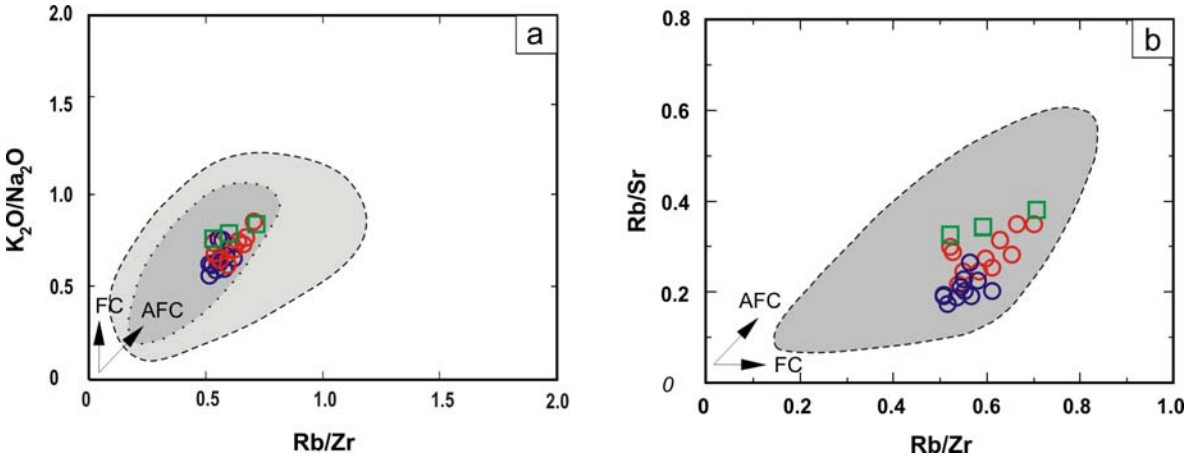

Fig. 7.2. Rb/Zr vs. K_2O/Na_2O (a) and Rb/Sr (b) variation diagrams for the quartz andesites from Oaş-Gutâi Mts. The dark grey fields represent the Gutâi Mts. volcanics (data from Kovacs & Fülöp, 2007) and the light grey field correspond to the Carpathian-Pannonian intermediate calc-alkaline volcanics (data from Seghedi *et al*., 2004). Symbols as in Fig. 6.1a.

- The presence of corroded cores and of sieved textures in the plagioclase phenocrysts due to the crystal-melt chemical disequilibrium as a consequence of the modification of the initial magma composition by magma mixing, as well as due to the temperature and pressure variations (Tepley III, 1999; Seaman, 1999);

- The presence of the recurrent oscillatory zoning and of the reverse zoning of the pyroxenes, which suggests changes in the crystallization conditions (P, T, chemistry) by magma mixing;

- The presence of rounded quartz crystals with resorbed rims, sometimes even with skeletal aspect, as well as the presence of the pyroxenes coronas around the quartz crystals from the „basic" quartz andesites, which are typical for magma mixing processes. These characteristic aspects of the quartz crystals suggest that they are xenocrysts taken from an acidic, more differentiated magma, where they originally formed.

The presence of the quartz phenocrysts along the high Mg# pyroxene phenocrysts and the high An plagioclases proves the mixing of magmas with different compositions (Nixon, 1988; Clynne, 1999; Murphy *et al.,* 2000) and the hybrid character of the quartz andesites rock-forming magmas.

CONCLUSIONS

The quartz andesites complex from the Oaş-Gutâi Mts. is a distinct stage in the evolution of the Neogene volcanism from this area. The mineralogical and geochemical data, provided by the electrone microprobe analysis and the major, minor and rare earth elements analysis, allowed the emphasis of some important features of these rocks:

- Oscillatory zoning, both normal and reverse of the plagioclase feldspars, with frequent recurrences and sieved textures;
- Normal and reverse zoning of the orthopyroxenes (enstatite and ferrosilite) and clinopyroxenes (augite and diopside);
- The presence of the magmatic amphibole (magnesio-hornblende);
- The presence of the rounded and frequently corroded quartz xenocrysts, sometimes with reaction pyroxene coronas;
- The calc-alkaline character of the generating magmas and the medium-K character of the quartz andesites;
- The enrichment in incompatible elements Rb, Ba, Th, U and K (LILE) and the depletion in Nb and Ta (HFSE);
- The enrichment in light rare earth elements (LREE) and the presence of the negative Eu anomaly.

All of the peculiarities emphasized for the quartz andesites complex are similar with those of the calc-alkaline rocks formed in the subduction zones. The nature of the magma sources can be considered of NMORB type, influenced to a higher degree by the composition of the sediments from the subducted slab compared with the fluids released from it.

The most important petrogenetic processes involved in the evolution of the parental magmas of the quartz andesites complex were the fractional crystallization, associated with crustal assimilation and magma mixing.

REFERENCES

Borcoş, M., Lang, B., Peltz, S., Stan, N. (1973). Volcanisme neogene des Monts Gutâi. *Rev. Roum. Géol*., 17(1), 81-93.

Cawthorn, R.G., Collerson, K.D. (1974). The recalculation of pyroxene end-member parameters and the estimation of ferrous and ferric content from electron microprobe analyses. *Amer. Mineral*., 59, 1203-1208.

Cioflică, Gr. (1956). Studiul geologic şi petrografic al formaţiunilor eruptive din regiunea Băiţa (Baia Mare). *An. Univ. Parhon, St. Nat*., 11, 233-251.

Clynne, M.A. (1999). Complex magma mixing origin for multiple volcanic lithologies erupted in 1915, from Lassen Peak, California. *J. Petrol*., 40, 105-132.

Csontos, L. (1995). Tertiary tectonic evolution of the Intra-Carpathian area: a review. *Acta Vulcanol*., 7, 1-13.

Csontos, L., Nagymarosy, A. (1998). The mid-Hungarian line: a zone of repeated tectonic inversion. *Tectonophysics*, 297, 51-71.

Csontos, L., Nagymarosy, A., Horváth, F., Kovác, W. (1992). Tertiary evolution of the Intra-Carpathian area: a model. *Tectonophysics*, 208, 221-241.

Deer, W.A., Howie, R.A., Zussman, J. (1992). An introduction to Rock Forming Minerals-2nd Edition. Longmans Group Ltd., London, 696 p.

De Paolo, J.D. (1981). Trace element and izotopic effects of combined wallrocks assimilation and fractional crystallization. *Earth Planet. Sci. Lett*., 53, 189-202.

Dimitrescu, R. (1954). Cercetări geologice în regiunea Capnic-Jereapăn (Baia Mare). *D.S. Com. Geol*., XXXVIII, 4-8.

Edelstein, O., Iştvan, D., Bernad, A., Kovacs, M., Stan, D., Catrina, F. (1982). Probleme actuale şi de perspectivă ale prospecţiunilor geologice din munţii Oaş-Ţibleş. *Vol. Carpaţii Orientali, Simp. Geol. I,* p. 205-219, Gheorgheni.

Edelstein, O., Răduţ, M., Istvan, D., Kovacs, M., Bernad, A., Gabor, M., Haranth, G. (1987). Intrusive bodies in the Oaş-Văratec Mountains and their relations to volcanic and to non-ferous mineralizations. *D.S. Inst. Geol. Geofiz.,* 72-73(1), 67-79.

Edelstein, O., Bernad, A., Kovacs, M., Crihan, M., Pécskay, Z. (1992a). Preliminary data regarding the K-Ar ages of some eruptive rocks from Baia Mare Neogene volcanic zone. *Rev. Roum. Géol*., 36, 45-60.

Edelstein, O., Iştvan, D., Kovacs, M., Bernad, A., Stan, D., Iştvan, E., Gabor, M., Balint, B., Haranth, G., Vârşescu, I. (1992b). Donnees preliminaires concernant la constitution geologique de la zone Săpânţa-Valea Brazilor (Monts de Igniş). *Rom J. Petrol*., 75, 131-143.

Edelstein, O., Péskay, Z., Kovacs, M., Bernad, A., Crihan, M., Micle, R. (1993). The age of the basalts from Firiza zone, Igniş Mts., East Carpathians, Romania. *Rev. Roum. Géol*., 37, 37-41.

Fülöp, A. (2001). A paleocaldera, source of 15.4 Ma rhyolitic ignimbrites from Gutai Mts, Eastern Carpathians, Romania. *European Science Foundation Project "Pannonian Basin, Carpathian and Dinaride System - PANCARDI", Geological Meeting on Dynamics of Ongoing Orogeny*, Abstracts, p. CO-6, Sopron.

Fülöp, A. (2002). Facies analysis of the volcaniclastic sequence built up above the 15.4 Ma rhyolitic ignimbrites from Gutai Mts., Eastern Carpathians. *Studia Univ. Babeş-Bolyai, Geol.,* Special issue, 1, 199-206.

Fülöp, A. (2003). The beginning of the volcanism in Gutâi Mts. Paleovulcanological and paleosedimentological reconstructions. *Ed. Dacia, Cluj-Napoca*, 134 p. (in Romanian)

Fülöp, A., Crihan, M. (2002). Badenian and Sarmatian acidic vulcanoclastics of pyroclastic origin from Oaş Mts., Eastern Carpathians (Northwestern România). *Rev. Roum. Géol*., 46, 61-72.

Fülöp, A., Kovacs, M. (1996). Pannonian acid volcanism in Gutâi Mts. (East Carpathians, Romania). Volcanological features, magmatological and tectonical significance. *In „Plate tectonic aspects of the alpine metallogeny in the Carpatho-Balkan region" UNESCO-IGCP Project 356, Proceed. annual meeting,* vol. 2, p. 57-67, Sofia.

Fülöp, A., Kovacs, M., Damian, F. (1991). Contributions to the petrographical study of the rhyodacitic Badenian volcano-sedimentary formation from the Purcăreţ and Puturoasa zones (Gutâi Mountains). *In „The volcanic tuffs from the Transilvanian Basin, Romania", Cluj-Napoca University, Geology-Mineralogy Department Special Issues,* p. 245-251, Cluj-Napoca.

Gill, J.B. (1981). Orogenic andesites and plate tectonics. Springer Verlag, New York, 370 p.

Giuşcă, D. (1960). The adularisation of the volcanics from the Baia Mare region. *Stud. Cerc. Geol*., V (3), 499-507.

Hawkesworth, C.J., Turner, S., Peate, D., McDermot, F., van Calsteren, P. (1997). Elemental U and Th variation in island arc rocks: implication for U-series isotopes. *Chem.l Geol*., 139, 207-221.

Hunter, A. G., Blake, S. (1995). Petrogenetic evolution of a transitional tholeitic-calc-alkaline series: Towada volcano, Japan. *J. Petrol*., 36, 1579-1605.

Ianovici, V., Giuşcă, D., Manilici, V., Gherasi, N., Jude, R., Gheorghiţă, I., Dimitrescu, R. (1961). Ghidul excursiilor. A - Baia Mare, *Asoc. Geol. Carp.-Balc. (Congr. al V-lea),* 55 p., Bucureşti

Jurje, M., Ionescu, C., Hoeck, V. (2010) Neogene quartz andesites from the Oaş-Gutâi Mts. (Romania): new geochemical data. *Acta Mineral. Petrogr*., 6, p. 520.

Jurje, M., Ionescu, C., Hoeck, V., Kovacs, M. (2011). New geochemical data on Neogene quartz andesites from the Oaş-Gutâi Mts., Eastern Carpathians, Romania *(in review*).

Jurje, M., Ionescu, C., Hoeck, V., Kovacs, M. (2011). Mineral chemistry of plagioclases from quartz andesites in Oaş-Gutâi Mts. *(in prep.)*

Kimura, J.I., Yoshida, T. (2006). Contributions of slab fluid, mantle wedge and the crust to the origin of Quaternary lavas in the NE Japan arc. *J. Petrol*., 47 (11), 2185-2232.

Kovacs, M. (2002). Petrogenesis of the subduction magmatic rocks from central-southeastern area of Gutai Mountains. Edit. Dacia Cluj-Napoca; 202 p. (in Romanian).

Kovacs, M., Fülöp, A. (2002). Neogene volcanism in Oaş Mts., Eastern Carpathians, Romania. *Geol. Carpath*., 53, 208-210.

Kovacs, M., Fülöp, A. (2003). Neogene volcanism in Gutâi Mts. (Eastern Carpathians). A review. *Studia Univ. Babeş-Bolyai, Geol*., XLVIII (1), 3-16.

Kovacs, M., Fülöp, A. (2010b). Mixing and mingling processes inthe Neogene volcanic rocks from Gutâi Mts. (NW Romania). Conferinţa Naţională a SGR Bucureşti, Abstracts Vol., CD-ROM.

Kovacs, M., Edelstein, O., Iştvan, D. (1987a). Andesites from Oaş-Ţibleş Mts.: Considerations regarding their definition and classification based on petrochemical data. *Stud. Cerc. Geol*., 32, 12-24. (in Romanian).

Kovacs, M., Edelstein, O., Iştvan, D., Pop, N., Bernad, A., Stan, D. (1987b). Petrological data on intrusive bodies from south-estern part of Oaş-Ţibleş Neogene volcanic chain (between Firiza- Valley. *D.S. Inst. Geol. Geof.*, 72-73(1), 97-119. (in Romanian).

Kovacs, M., Edelstein, O., Iştvan, D., Grabari, G., Stoian, M., Popescu, Gh. (1992). Distribution of REE, K, Rb, Sr and $^{87}Sr/^{86}Sr$ ratios in the Neogene andesites of the Igniş-Văratec (Gutâi) Mountains. *Rom. J. Petrol*., 75, 145-159.

Kovacs, M., Pécskay, Z., Edelstein, O., Crihan, M., Bernad, A., Gabor, M. (1995). The evolution of the magmatic activity in the Poiana Botizei-Ţibleş area; a new approach based on radiometric datings. Mineralogical Society of Romania - Third symposium on Mineralogy, Abstracts vol., *Rom. J. Mineral.,* 77 (1), p. 25.

Kovacs, M., Pécskay, Z., Crihan, M., Edelstein, O., Gabor, M., Bernad, A. (1997a). K-Ar study of neogene volcanic rocks from the Oaş Mts. (East Carpathians, Romania), *Rev. Roum. Géol*., 41, 19-28.

Kovacs, M., Edelstein, O., Gabor, M., Bonhomme, M., Pécskay, Z. (1997b). Neogene magmatism and metallogeny in Oaş-Gutâi-Ţibleş Mts.; a new approach based on radiometric datings. *Rom. J. Miner. Dep.,* 78, 35-45.

Kovacs, M., Fülöp, A., Cook, N.J., Kovacs-Palffy, P., Pécskay, Z. (2010a). Magma mingling and mixing as key processes in the petrogenesis of the Laleaua Albă Neogene composite igneous complex, Gutâi volcanic zone, Northern Romania. *Acta Mineral. Petrogr*., 6, p. 520.

Kovacs, M., Pécskay, Z., Fülöp, A., Jurje, M., Edelstein, O. (2010b). Time and space distribution of the Neogene intrusive magmatism from Oaş-Gutâi Mts., Eastern Carpathians, Romania. *Geologica Balcanica*, 39 (1-2), 214-215.

Kovács, S. (1982). Problems of the "Pannonian Median Massif" and the plate tectonic concept. Contributions based on the distribution of Late Paleozoic–Early Mesozoic isotopic zones. *Geol. Rund*., 71 (2), 617-639.

Lang, B., Edelstein, O., Steinitz, G., Kovacs M., Halga S. (1994). Ar-Ar dating of adularia - a tool in understanding genetic relation between volcanism and mineralization: Baia Mare area (Gutâi Mountains), northwestern România. *Econ. Geol*., 89, 174-180.

Leake, B.E. (1997). Nomenclature of amphiboles: Report of the subcommittee on amphiboles of the International Mineralogical association, commission on new minerals and minerals names. *Can. Mineral*., 35, 219-246.

Le Maître, R.W., Bateman P., Dudek, A., Keller, J., Lameyre Le Bas, M.J., Sabine, P.A., Schmid, R., Sorensen, H., Streckeisen, A., Woolley, A.R., Zanettin, B. (1989). A classification of igneous rocks and a glossary of terms. *Blackwell, Oxford*, 193 p.

Lexa, J., Konečny, V. (1998). Geodynamic aspects of the Neogene to Quaternary volcanism*. In: Rakus, M. (Ed.), Geologic Development of the Western Carpathians. GSSR, Bratislava*, p. 219– 240.

Márton, E., Pogác, P., Túnyi, I. (1992). Paleomagnetic investigations on Late Cretaceous-Cenozoic sediments from the NW part of the Pannonian Basin. *Geol. Carpath*., 43, 363-369.

Mason, P.R.D., Seghedi, I., Szakacs, A., Downes, H. (1998). Magmatic constraints on geodynamic models of subduction in the Eastern Carpathians, Romania. *Tectonophysics*, 297, 157-176.

Morimoto, N. (1988). Nomenclature of pyroxene. *Can. Mineral*., 27, 143-156.

Murphy, M.D., Sparks, R.S.J., Barclay, J., Carroll, M.R., Brewer, T.S. (2000). Remobilization of andesite magma by intrusion of mafic magma at the Soufriere Hills Volcano, Montserrat, West Indies. *J. Petrol*., 41, 21-42.

Nelson, S.T., Montana, A. (1992). Sieve-textured plagioclase in volcanic rocks produced by decompression. *Amer. Mineral*., 77, 1242-1249.

Nemčok, M., Pospisil, L., Lexa, J., Donelik, R.A. (1998). Tertiary subduction and slab breakoff model of the Carpathian Pannonian region. *Tectonophysics*, 295, 307– 340.

Nixon, T.G. (1988). Petrology of the younger andesites and dacites of Iztaccihuatl Volcano, Mexico: I. Disequilibrium phenocryst assemblages as indicators of magma chamber process. *J. Petrol*., 29, 213-264.

Panaiotu, C., Pécskay, Z., Panaiotu, C.E. (1996). Which is the time of rotation? Review of paleomagnetic and and K-Ar data from Romania. *Mitt. Ges. Geol. Bergbaustud. Osterr*., 41, p. 125.

Pătraşcu, S., Panaiotu, C., Şeclăman, M., Panaiotu, C.E. (1994). Timing and rotational motions of Apuseni Mountains, Romania: paleomagnetic data from Tertiary magmatics rocks. *Tectonophysics*, 233, 163-176.

Peresson, H., Deker, H. (1997). Far field effects of Late Miocene subduction in the Estern Carpathians: E-W compression and inversion of structures in the Alpine-Carpatho-Pannonian region. *Tectonics*, 16, 38-56.

Pécskay, Z., Edelstein, O., Kovacs, M., Bernad, A., Crihan, M. (1994). K-Ar age determination of Neogene volcanic rocks from the Gutâi Mts. (Eastern Carpathians, Romania). *Geol. Carpath*., 45 (6), 357-363.

Pécskay, Z., Edelstein, O., Seghedi, I., Szakacs, A., Kovacs, M., Crihan, M., Bernad, A. (1995a). K-Ar datings of Neogene-Quaternary calc-alkaline volcanic rocks in Romania. *Acta Vulcanol*., 7, 53-62.

Pécskay, Z., Lexa, J., Szakacs, A., Balogh, K., Seghedi, I., Konečny, V., Kovacs, M., Marton, M., Kaliciak, M., Szeky-Fux, V., Poka, T., Gyarmaty, P., Edelstein, O., Roşu, E., Zec, B. (1995b). Space and time distribution of Neogene - Quaternary volcanism in the Carpatho-Pannonian region. *Acta Vulcanol*. 7, 15-29.

Pécskay, Z., Lexa, J., Szakacs, A., Seghedi, I., Balogh, K., Konečný, V., Zelenka, T., Kovacs, M., Poka, T., Fülöp, A. (2004). Geochronology of Neogene-Quaternary magmatism in the Carpathian-Pannonian Region. A review. *32nd Intern. Geol.l Congr., Abstr*., 2, p. 1245, Florence.

Pécskay, Z., Lexa, J., Szakacs, A., Seghedi, I., Balogh, K., Konečny, V., Zelenka, T., Kovacs, M., Poka, T., Fülöp, A., Marton, E., Panaiotu, C., Cvetković, V. (2006). Geochronology of Neogene magmatism in the Carpathian arc and intra-Carpathian area: a review. *Geol. Carpath*., 57 (6), 511-530.

Pécskay, Z., Seghedi, I., Kovacs, M., Szakács, A., Fülöp, A. (2009). Geochronology of the Neogene calc-alkaline intrusive magmatism in the "Subvolcanic Zone" of the Eastern Carpathians (Romania). *Geol. Carpath*., 60 (2): 181-190.

Rădulescu, D. (1958). Petrographical study of the igneous formations from Seini-Ilba-Nistru (Baia Mare) region. *An. Com. Geol*., XXXI, 151-260.(in Romanian).

Rădulescu, D., Borcoş, M. (1969). Apércu général sur l'evolution du volcanisme néogene en Roumanie. *An. Com. Stat Géol*., XXXVI, 177-193.

Rădulescu, D., Săndulescu, M., Borcoş, M. (1993). Alpine magmatogenic map of Romania: an approach to the systematization of the igneous activity. *Rev. Roum. Géol*., 37, 3-8.

Robinson, P., Spear, F.S., Schumacher, J.C., Laird, J., Klein, C., Evans, B.V., Doolan, B.L. (1981). Phase relations of metamorphic amphiboles: Natural occurence and theory. *Rev. Mineral*., 9B, 1-228.

Sagatovici, A. (1968). Studiul geologic al părţii de vest şi centrale a Bazinului Oaş*; Stud. Tehn. Econ*., 5, 7-146.

Săndulescu, M. (1984). The geotectonics of Romania. Bucharest: Ed. tehnică, Bucharest, 336 p. (in Romanian)

Săndulescu, M., Visarion, M., Stănică, D., Stănică, M., Atanasiu, L. (1993). Deep structure of the Inner Carpathians in the Maramureş-Tisa zone (East Carpathians). *Rom. J. Geophys*., 16, 67-76.

Seaman, S.J. (2000). Crystal clusters, feldspar glomerocrystsand magma envelopes in the Atascosa Lookout lava flow, Southern Arizona, USA: recorders of magmatic events. *J. Petrol.,* 41/5, 693-716.

Seghedi, I., Balintoni, I., Szakács, A. (1998). Interplay of tectonics and Neogene post-collisional magmatism in the intracarpathian region. *Lithos*, 45, 483-499.

Seghedi, I., Downes, H., Szakács, A., Mason, P.R.D., Thirlwall, M.F., Roşu, E., Pécskay, Z., Márton, E., Panaiotu, C. (2004). Neogene-Quaternary magmatism and geodynamics in the Carpathian–Pannonian region: a synthesis. *Lithos*, 72, 117-146.

Seghedi, I., Downes, H., Harangi, S., Mason, P.R.D., Pécskay, Z. (2005). Geochemical response of magmas to Neogene-Quaternary continental collision in the Carpathian–Pannonian region: A review. *Tectonophysics,* 410, 485-499.

Singer, B.S., Dungan, M.A., Layne, G.D. (1995). Textures and Sr, Ba, Mg, Fe, K and profiles in volcanic plagioclase: clues to the dynamics of calc-alkaline magma chambers. *Amer. Mineral*., 80, 776-798.

Sun, S.S., McDonough, W.F. (1989). Chemical and isotopic systematics of oceanic basalts: implication for mantle compositions and processes. *Geol. Soc. London, Sp. Publ*.,42, 313-345.

Szabó, Cs., Harangi, Sz., Csontos, L. (1992). Review of Neogene and Quaternary volcanism of the Carpathian–Pannonian region. *Tectonophysics*, 208, 243-256.

Tepley III, F.J., Davidson, J.P., Clynne, M.A. (1999). Magmatic interactions as recorded in plagioclase phenocrysts of Chaos Crags, Lassen Volcanic Center, California. *J. Petrol*., 40 (5), 787-806.

Tischiler, M., Groger, H.R., Fugenschuh, B., Schmit, S.M. (2007). Miocene tectonics of the Maramures area (Northern Romania): implication for the Mid-Hungarian fault zone. Intern. *Jour. Earth Sci*., 96, 473-496.

Toothill, J., Williams, C.A., Macdonald, R., Turner, S.P., Rogers, N.W., Hawkesworth, C.J., Jerram, D.A., Ottley, C.J., Tindle, A.G. (2007). A complex petrogenesis for an arc magmatic suite, St Kitts, Lesser Antilles. *J. Petrol*., 48 (1), 3-42.

Wilson, M. (1989). Igneous Petrogenesis. Wiley, London, 466 p.

Zellmer, G.F., Hawkesworth, C.J., Sparks, R.S.J. Thomas, L.E., Harford, C.L., Brewer, T.S., Loughlin, S.C. (2003). Geochemical evolution of the Soufrière Hills Volcano, Montserrat, Lesser Antilles volcanic Arc. *J. Petrol*., 44 (8), 1349-1374.